# THEORETICAL INVESTIGATION OF MINIMUM TIME LOOP MANEUVERS OF JET AIRCRAFT

Thesis by

Sachio Uehara

In Partial Fulfillment of the Requirements

For the Degree of

Doctor of Philosophy

California Institute of Technology

Pasadena, California

1974

(Submitted May 3, 1974)

ACKNOWLEDGEMENTS

The author wishes to express his appreciation to Dr. Homer J. Stewart, his advisor, for guidance and encouragement through the course of this research. He is also indebted to Dr. Lincoln J. Wood for many helpful discussions and suggestions. Thanks are also due to Mrs. Virginia Anderson for acquisition of reference material, Mrs. Jacquelyn Beard for typing of the manuscript, and Mrs. Betty Wood for drawing the figures.

The financial support of the California Institute of Technology in the form of a Scholarship, Graduate Teaching Assistantship, Fellowship, and computing fund is gratefully acknowledged.

# ABSTRACT

Minimum time loop maneuvers of high performance jet aircraft have been investigated by means of the calculus of variations. A number of simplifying assumptions have been made in the atmospheric conditions, aerodynamic parameters, and the number of controls and their upper and lower bounds, in order to obtain general features and basic characteristics of the problem. The optimal control (lift coefficient and thrust) has been determined as a function of the state variables and Lagrange multipliers. It is found that subarcs with variable thrust, or with variable lift coefficient and minimum thrust do not occur on time optimal paths. Possible transitions among the five optimal subarcs have been established by applying the corner conditions of variational calculus. These relationships are applicable to any minimum time maneuver in the vertical plane. The effects of the magnitudes of maximum lift coefficient and maximum thrust on the control program, maneuver time, final speed, and final horizontal distance for minimum time loop maneuvers are explored through numerical computation. It is found that the control history in lift and thrust and the minimum time required for a loop maneuver depend strongly on the magnitudes of maximum lift coefficient and maximum thrust.

A limited numerical exploration using more realistic aerodynamic and atmospheric parameters and a state-dependent maximum thrust yielded results in qualitative agreement with the more extensive analysis based on simplified parameters. Normal

acceleration constraints are analyzed by considering the maximum lift coefficient to be a function of altitude and speed. New design criteria for the inlet, duct and engine are suggested by consideration of the problem of engine surge.

# TABLE OF CONTENTS

TABLE OF CONTENTS (Cont'd)

# LIST OF SYMBOLS

| Symbol | Definition |
|---|---|
| a | Speed of sound |
| $C_D$ | Drag coefficient = $C_{D0} + KC_L^2$ |
| $C_{D0}$ | Zero-lift drag coefficient |
| $C_L$ | Lift coefficient |
| D | Drag of aircraft = $\frac{1}{2}\rho V^2 S C_D = \frac{1}{2}\varkappa p M^2 S C_D$ |
| g | Acceleration of gravity |
| G | Function of end coordinates to be optimized |
| $h_e$ | Energy height = $y + \frac{V^2}{2g}$ |
| H | Variational Hamiltonian |
| I | Performance index to be optimized |
| K | Airplane efficiency factor |
| L | Lift of aircraft = $\frac{1}{2}\rho V^2 S C_L = \frac{1}{2}\varkappa p M^2 S C_L$ |
| M | Mach number of forward velocity = $\frac{V}{a}$ |
| n | Load factor (Normal acceleration in g's) |
| p | Atmospheric pressure |
| $p_0$ | Atmospheric pressure at the reference altitude |
| q | Dynamic pressure = $\frac{1}{2}\rho V^2 = \frac{1}{2}\varkappa p M^2$ |
| S | Wing area of aircraft |
| Sw | Reciprocal of dimensionless wing loading = $\frac{\varkappa p_0 S}{2W}$ |
| t | Time |
| T | Thrust |
| Tw | Thrust to weight ratio = $\frac{T}{W}$ |
| u | Column vector of control variables |

LIST OF SYMBOLS (Cont'd)

| Symbol | Definition |
|---|---|
| $V$ | Forward velocity of aircraft |
| $W$ | Weight of aircraft |
| $x$ | Range, Horizontal distance |
| $y$ | Altitude |
| $z$ | Column vector of state variables |
| $\alpha$ | Angle of attack |
| $\gamma$ | Flight path angle |
| $\eta$ | Dimensionless altitude = $\frac{gy}{a^2}$ |
| $\varkappa$ | Ratio of specific heats of air = 1.4 |
| $\lambda$ | Column vector of Lagrange multipliers |
| $\lambda_j$ | j-th Lagrange multiplier for differential constraint |
| $\mu_j$ | j-th Lagrange multiplier for inequality constraint |
| $\xi$ | Dimensionless range = $\frac{gx}{a^2}$ |
| $\rho$ | Atmospheric density |
| $\tau$ | Dimensionless time = $\frac{gt}{a}$ |
| $(\dot{})$ | Derivative with respect to time |
| $(\,)'$ | Derivative with respect to dimensionless time |
| $(\,)^T$ | Transpose of vector |
| $(\,)_c$ | Value at a corner point |
| $(\,)_f$ | Final value |
| $(\,)_i$ | Initial value |
| $(\,)_i^f$ | Difference between final and initial values = $(\,)_f - (\,)_i$ |
| $(\,)_N$ | Value corresponding to minimum load factor |

LIST OF SYMBOLS (Cont'd)

| Symbols | Definition |
|---|---|
| $( )_X$ | Value corresponding to maximum load factor |
| $( )_{AVG}$ | Average of maximum and minimum values $= \frac{1}{2}\left[ ( )_{MAX} + ( )_{MIN} \right]$ |
| $( )_{INT}$ | Intermediate value |
| $( )_{MAX}$ | Maximum value |
| $( )_{MIN}$ | Minimum value |
| $( )_+$ | Value just after a corner point |
| $( )_-$ | Value just before a corner point |

# LIST OF TABLES

# LIST OF FIGURES

LIST OF FIGURES (Cont'd)

LIST OF FIGURES (Cont'd)

# I. INTRODUCTION

In recent years, optimal control theory has been applied to various performance optimization problems associated with high speed aircraft. Minimum time and minimum fuel climbs have been investigated by Miele and Capellari (1), Cicala and Miele (2), Landgraff (3), Bryson, Desai, and Hoffman (4), and others. Bryson, Desai, and Hoffman (4) and Miele (5) have analyzed the problems of range maximization and endurance maximization with a given quantity of fuel. Constant altitude and three-dimensional minimum time and minimum fuel turns have been treated by Bryson and Lele (6), Hedrick and Bryson (7,8,9), Hoffman, Zvara, and Bryson (10), and others. Parsons, et al., analyzed constant altitude and three-dimensional minimum time turns to a point and onto a line in Ref. 11, 12 and 13.

In this thesis, loop maneuvers are considered. A loop maneuver is an aerial maneuver in which the aircraft describes an approximately circular path in the vertical plane. Normally, the upper surface of the aircraft remains on the inside of the circle and the lateral axis of the aircraft remains horizontal. The flight path, which begins at angle of climb of $0^{o}$ and ends at $360^{o}$, is obtained mainly by lift and thrust control. This maneuver is to be performed within the speed-load factor envelope, subject to upper and lower bounds on the lift coefficient, thrust and zero-lift drag coefficient. Spintzyk (14) discussed this maneuver as a part of the target chasing maneuver. Vincent, et al., (15) investigated only the climbing part of such a maneuver.

The minimum time and radius of turn associated with a loop maneuver are useful indices in evaluating the maneuverability of a high performance aircraft in the vertical plane. This maneuver includes a steep climb and descent with a large normal acceleration, as well as flight at a high angle of attack. It is therefore useful in training pilots. This maneuver is performed in aerial combat as a target chasing or evasive maneuver.

In a loop maneuver, pilots are interested in the control program, the loss of speed and altitude, the fuel consumption, and the number of changes in control required for the completion of a minimum time maneuver. Designers are interested in the effects of the thrust to weight ratio, the wing loading, the maximum lift coefficient, etc., on the overall optimal loop maneuver.

In this thesis, the minimum time loop maneuver of high performance aircraft will be investigated from the viewpoints of both the pilot and the designer. In Part II, the basic optimization problem is formulated, after a number of simplifying assumptions have been made. The optimal control is determined as a function of the state variables and Lagrange multipliers, using the minimum principle. The possibility of singular arcs is ruled out by the generalized Legendre-Clebsch condition. By applying the corner conditions of variational calculus, it is determined under what circumstances the control can switch from one mode to another. The results obtained in this part are applicable not only to minimum time loop maneuvers, but, in fact, to any minimum time maneuver in the vertical plane.

In Part III, numerical methods for determining optimal trajectories, subject to a variety of terminal conditions, are discussed. In Part IV, the effects of the upper limits on the lift coefficient and thrust are analyzed. The control history and the minimum time required for a loop maneuver are found to depend strongly on the upper bounds placed upon the control variables. Concluding remarks are made in Part V.

# II. ANALYTICAL FORMULATION

## 2.1 Equations of Motion and Simplifying Assumptions

The forces acting on an aircraft moving in the vertical plane are shown in Fig. 1. If the aircraft is modelled as a point mass, the equations of motion are (16)

$$\frac{W}{g}\dot{V} = T\cos\alpha - D - W\sin\gamma$$

$$\frac{W}{g}V\dot{\gamma} = T\sin\alpha + L - W\cos\gamma$$

$$\dot{x} = V\cos\gamma$$

$$\dot{y} = V\sin\gamma$$

The transient forces due to changes in lift control have been neglected since the duration of such forces is very short compared with the length of the maneuver (see Appendix A). It has been assumed that the thrust direction coincides with the aircraft longitudinal reference axis.

There are several approximations which may be used to analyze motion in the vertical plane (4). The quasi-steady approximation (as defined in Ref. 4), in which accelerations are neglected completely, is adequate for treating the climb performance of subsonic aircraft. However, this approximation is inadequate for a loop maneuver, which requires changes in flight path angle of $360^{o}$. The energy-state approximation, in which energy is the only state variable, is quite useful for analyzing the minimum time and maximum range performance of high speed aircraft, provided that the acceleration normal to the flight path can be neglected, and provided that the flight is nearly horizontal. In a loop maneuver

neither of these assumptions is justified. A more accurate approximation involves considering the velocity and altitude as state variables and the flight path angle as a control variable. This approach is also not suitable for analysis of a loop maneuver, since acceleration normal to the flight path is again neglected. Since accelerations parallel to and normal to the flight path are much more important in a loop maneuver than in a climb, the selection of velocity, flight path angle and altitude as state variables, and lift coefficient, thrust and zero-lift drag coefficient as control variables is appropriate for analysis of a loop maneuver.

Constraints on the state variables and control variables which may have to be considered are the following:

$$0 < M \leq M_{MAX}$$

$$n_{MIN} \leq n \leq n_{MAX}$$

$$C_{L_{MIN}} \leq C_L \leq C_{L_{MAX}}$$

$$T_{MIN} \leq T \leq T_{MAX}$$

$$C_{D0_{MIN}} \leq C_{D0} \leq C_{D0_{MAX}} \quad .$$

Control variables are lift, thrust and drag.

The objective is to obtain the minimum time control history for a loop maneuver subject to the constraints described above. This problem is expressible as a Mayer problem of variational calculus (17, 18, 19). The Mayer problem involves minimizing a function of the initial and terminal states and times,

$$I = [G\ (t,\ z)]_i^f$$

subject to various path and endpoint constraints. In this case $G = t$ .

To reduce the complexity of the problem and to determine the general features of its solution, the following simplifying assumptions have been made:

1) The atmosphere is isothermal.
2) The angle of attack is small, so that $\cos\alpha \simeq 1$ and $\sin\alpha \simeq \alpha$ .
3) The thrust component in the lift direction is much smaller than the lift, i.e., $T\alpha \ll L$ .
4) The weight of the aircraft is constant.
5) The atmospheric pressure is constant.
6) $C_{D0}$ is constant. No drag control is considered.
7) The normal acceleration and Mach number are unconstrained.
8) $C_{L_{MAX}}$, $C_{L_{MIN}}$, $T_{MAX}$, $T_{MIN}$ are all constant.

The equations of motion may be transformed into dimensionless form by introducing the dimensionless variables:

$$\tau = \frac{gt}{a}\ ,\ Tw = \frac{T}{W}\ \text{(new control variable)}$$

$$Sw = \frac{\rho p_0 S}{2W}\ ,\ \xi = \frac{gx}{a^2},\ \eta = \frac{gy}{a^2}\ .$$

The state equations, control constraints, and peformance index may be expressed as follows:

$$M' = Tw - Sw\, M^2 \,(C_{D0} + KC_L{}^2) - \sin\gamma \tag{1-1}$$

$$\gamma' = \frac{1}{M}(Sw\, M^2\, C_L - \cos\gamma) \tag{1-2}$$

$$\xi' = M\cos\gamma \tag{1-3}$$

$$\eta' = M\sin\gamma \tag{1-4}$$

$$(C_L - C_{L_{MAX}})\,(C_L - C_{L_{MIN}}) \le 0 \tag{1-5}$$

$$(Tw - Tw_{MAX})(Tw - Tw_{MIN}) \le 0 \tag{1-6}$$

$$I = [\tau]_i^f \tag{1-7}$$

Eq. (1-1) explicitly assumes the drag coefficient $C_D$ to be a parabolic function of $C_L$, i.e., $K = (1/2C_L)(\partial C_D/\partial C_L)$ is assumed to be a constant (possibly varying with Mach number). In the following analysis, it is assumed that $K$ is chosen to make a good empirical approximation and the resulting small variation of $K$ with $C_L$ is neglected.

## 2.2 Analysis by the Calculus of Variations

The variational Hamiltonian of the system may be constructed by introducing Lagrange multipliers:

$$H = \lambda_1 [\, Tw - Sw\, M^2 \,(C_{D0} + KC_L{}^2) - \sin\gamma)]$$
$$+ \frac{\lambda_2}{M}(Sw M^2 C_L - \cos\gamma) + \lambda_3 M\cos\gamma + \lambda_4 M\sin\gamma \quad .$$

The Euler-Lagrange equations, which are expressible in general form as

$$(\lambda')^T = -\frac{\partial H}{\partial z}$$

become

$$M: \lambda_1' = \lambda_1 2SwMC_D - \frac{\lambda_2}{M^2}(SwM^2C_L + \cos\gamma) - \lambda_3\cos\gamma$$

$$-\lambda_4 \sin\gamma \qquad (2\text{-}1)$$

$$\gamma: \lambda_2' = \lambda_1\cos\gamma - \frac{\lambda_2}{M}\sin\gamma + \lambda_3 M\sin\gamma - \lambda_4 M\cos\gamma \qquad (2\text{-}2)$$

$$\xi: \lambda_3' = 0 \Rightarrow \lambda_3 = \text{constant} \qquad (2\text{-}3)$$

$$\eta: \lambda_4' = 0 \Rightarrow \lambda_4 = \text{constant} \qquad (2\text{-}4)$$

H is not an explicit function of $\tau$ ; consequently a first integral of motion exists - the Hamiltonian is constant. The transversality condition

$$\left(\frac{\partial I}{\partial \tau} + H\right)_{\tau=\tau_f} = 0$$

yields

$$H = \lambda_1 (Tw - SwM^2C_D - \sin\gamma) + \frac{\lambda_2}{M}(SwM^2C_L - \cos\gamma)$$

$$+ \lambda_3 M\cos\gamma + \lambda_4 M\sin\gamma = -1 \qquad (2\text{-}5)$$

In this problem it is expected from the inequality constraints on the control variables that there are several subarcs corresponding to qualitatively different types of control behavior, which may be joined together to construct an optimal flight path. Since there are no interior point constraints, the following corner conditions must be satisfied at the junction of two subarcs

$$(H)_- = (H)_+ \qquad (2\text{-}6)$$

$$(\lambda)_- = (\lambda)_+ \quad , \qquad (2\text{-}7)$$

i.e., the first integral and each of the Lagrange multipliers is continuous at each corner.

2.3 Characteristics of Subarcs

Optimal controls will be determined by using the minimum principle*. The control variables $C_L$ and Tw are not coupled in H. Hence, H may be optimized with respect to each control variable independently. Since H is linear in Tw, H is minimized with respect to Tw when

$$Tw = \begin{cases} Tw_{MAX} \text{ if } \lambda_1 < 0 , \\ Tw_{INT} \ (Tw_{MIN} < Tw < Tw_{MAX}) \text{ if } \lambda_1 = 0 \text{ (for finite time interval),} \\ Tw_{MIN} \text{ if } \lambda_1 > 0 . \end{cases}$$

An arc with $Tw = Tw_{INT}$ is a singular arc, since $\partial H/\partial Tw = \lambda_1 = 0$ and $\partial^2 H/\partial Tw^2 = 0$ on this arc. Additional tests are needed to determine whether such an arc can be optimal. Since $\lambda_1 \equiv 0$ on this arc, it follows that

$$\frac{d}{d\tau}\left(\frac{\partial H}{\partial Tw}\right) = \lambda_1' = 0.$$

Eqs. (2-1) and (2-5) imply that

$$\lambda_1' = \frac{1}{M}\left(1 - \frac{2\lambda_2 \cos\gamma}{M}\right) = 0$$

---

*The minimum principle states that the optimal control at each point along a trajectory is that value which globally minimizes H over the set of all admissible controls, with the state, Lagrange multipliers and time regarded as constant (20).

or

$$2\lambda_2 \cos\gamma = M \ . \tag{3-1}$$

Furthermore,

$$\frac{d^2}{d\tau^2}\left(\frac{\partial H}{\partial Tw}\right) = \lambda_1'' = \left(\frac{4\lambda_2 \cos\gamma - M}{M^3}\right) Tw + \text{other terms not involving } Tw \ . \tag{3-2}$$

The generalized Legendre-Clebsch condition (20) requires that

$$\frac{\partial}{\partial Tw}\left[\frac{d^2}{d\tau^2}\left(\frac{\partial H}{\partial Tw}\right)\right] \leq 0 \ ,$$

i.e., $1/M^2 \leq 0$ from Eqs. (3-1) and (3-2). Since $M$ must be real, the generalized Legendre-Clebsch condition is not satisfied. Hence, intermediate thrust arcs are not optimal.

$H$ is stationary with respect to $C_L$ when

$$\frac{\partial H}{\partial C_L} = Sw M \left(-2\lambda_1 K C_L M + \lambda_2\right) = 0 \ . \tag{3-3}$$

From Eq. (3-3), it may be observed that $H$ is stationary if

$$\lambda_1 = \lambda_2 = 0 \quad ,$$

$$C_L = \frac{\lambda_2}{2KM\lambda_1} \ , \tag{3-4}$$

or $\quad C_L = \lambda_2 = 0 \ .$

2.3.1 $\lambda_1 = \lambda_2 = 0$

If $\lambda_1 = 0$ for a finite period of time, a singular arc with intermediate thrust exists. This has been shown above to be non-optimal. Hence, $\lambda_1$ and $\lambda_2$ can both vanish only at isolated points.

2.3.2 $C_L = \dfrac{\lambda_2}{2KM\lambda_1}$

Since H is quadratic in $C_L$, the above choice of $C_L$ minimizes H if $\lambda_1 < 0$ and maximizes H if $\lambda_1 > 0$ (see Fig. 2). This value of $C_L$ may be within the allowable range of $C_L$, or outside of it. It is now easy to deduce the optimal value of $C_L$ subject to Eq. (1-5), according to the location of this stationary point and the sign of $\lambda_1$.

For the case in which $\lambda_1 < 0$ ($Tw = Tw_{MAX}$), the choice of $C_L$ which minimizes H is the following:

$$\frac{\lambda_2}{2KM\lambda_1} \geq C_{L_{MAX}} \Rightarrow C_L = C_{L_{MAX}},$$

$$C_{L_{MIN}} < \frac{\lambda_2}{2KM\lambda_1} < C_{L_{MAX}} \Rightarrow C_L = C_{L_{INT}} = \frac{\lambda_2}{2KM\lambda_1},$$

$$\frac{\lambda_2}{2KM\lambda_1} \leq C_{L_{MIN}} \Rightarrow C_L = C_{L_{MIN}}.$$

For the case in which $\lambda_1 > 0$ ($Tw = Tw_{MIN}$), choosing $C_L = \dfrac{\lambda_2}{2KM\lambda_1}$ maximizes H. In this case, a plot of H versus $C_L$ is concave downward as seen in Fig. 2. Thus H cannot have an unconstrained minimum with respect to $C_L$. The optimal choice of $C_L$ must be either $C_{L_{MAX}}$ or $C_{L_{MIN}}$, never an intermediate value. It is easy to show that the optimal choice of $C_L$ is as follows:

$$\frac{\lambda_2}{2KM\lambda_1} \begin{cases} < \dfrac{C_{L_{MAX}} + C_{L_{MIN}}}{2} \triangleq C_{L_{AVG}} & \Rightarrow C_L = C_{L_{MAX}} \\ > C_{L_{AVG}} & \Rightarrow C_L = C_{L_{MIN}}. \end{cases}$$

If $\frac{\lambda_2}{2KM\lambda_1} = C_{L_{AVG}}$, H has a double minimum with respect to $C_L$. $C_{L_{MAX}}$ and $C_{L_{MIN}}$ produce the same value of H.

2.3.3 $C_L = \lambda_2 = 0$

Although this nonlifting arc, which produces minimum drag and hence maximum excess power, is a special case of the intermediate lift arcs considered above, it will be investigated here, because of its special physical significance. The fact that the lift is intermediate implies that $\lambda_1 < 0$ ($Tw = Tw_{MAX}$) by the analysis in Sections 2.3.1 and 2.3.2. On this arc $\lambda_2' \equiv 0$ and

$$\gamma' = -\frac{\cos\gamma}{M} . \tag{3-5}$$

From Eqs. (2-2) and (3-5), we have

$$\lambda_1\gamma' = \lambda_3\sin\gamma - \lambda_4\cos\gamma .$$

Differentiation of the above equation with respect to $\tau$ gives

$$\lambda_1' + \frac{\gamma''}{\gamma'}\lambda_1 = (\lambda_3\cos\gamma + \lambda_4\sin\gamma).$$

This equation, together with Eqs. (2-1) and (2-5) yields the following equations,

$$M\lambda_1' + M\lambda_1\frac{\gamma''}{\gamma'} = \lambda_1 2SwM^2C_{D0} - M\lambda_1' \tag{3-6}$$

$$M\lambda_1' + M\lambda_1\frac{\gamma''}{\gamma'} = -1 - \lambda_1M' . \tag{3-7}$$

Consistency of Eqs. (3-6) and (3-7), in conjunction with Eqs. (1-1), requires that

$$\lambda_1 = \frac{-2}{Tw_{MAX} + SwM^2C_{D0}} , \tag{3-8}$$

where use has been made of the expression

$$\frac{\gamma''}{\gamma'} = -\frac{M'}{M} + \frac{\sin\gamma}{M} \tag{3-9}$$

from Eq. (3-5). Substitution of Eq. (3-9) into Eq. (3-7) gives

$$M\lambda_1' = -1 - \lambda_1 \sin\gamma \ . \tag{3-10}$$

Eqs. (3-8) and (3-10) should be both satisfied on this arc.

Differentiation of Eq. (3-8) and substitution into Eq. (3-10) yields the following functional relationship between $M$ and $\gamma$:

$$Tw_{MAX}^2 + 6Tw_{MAX}D_0 - 3D_0^2 - 6D_0\sin\gamma - 2Tw_{MAX}\sin\gamma = 0, \tag{3-11}$$

$$\text{where} \quad D_0 = SwM^2C_{D0} \ .$$

Since $M$ and $\gamma$ evolve in time according to Eqs. (1-1) and (1-2), Eq. (3-11) will generally be satisfied only at isolated points. Hence, an arc with $C_L = 0$ and $\lambda_2 = 0$ cannot exist.

Thus, there are five control modes (combinations of $Tw$ and $C_L$) which may be used to construct an optimal path. The optimal mode at time $\tau$ depends on $M(\tau)$, $\lambda_1(\tau)$ and $\lambda_2(\tau)$. The results of this analysis of subarcs are summarized in Table 1.

## 2.4 Intermediate Lift Program

For numerical solution of this variational problem, it is useful to obtain a differential equation which is satisfied by $C_L$ on intermediate lift arcs. This can be done by differentiating both sides of the expression

$$\lambda_2 = 2KC_LM\lambda_1 \tag{4-1}$$

with respect to $\tau$ . We obtain

$$\lambda_2' = \lambda_1' 2KC_L M + \lambda_2 2K\,(C_L' M + C_L M').$$

Substituting Eqs. (1-1), (2-1), (2-2) and (4-1) into the above equation gives the time derivative of the lift coefficient as

$$C_L' = \frac{1}{2KM}\left\{\frac{M}{\lambda_1}\left[\lambda_3(\sin\gamma + 2KC_L\cos\gamma) - \lambda_4(\cos\gamma - 2KC_L\sin\gamma)\right]\right.$$
$$\left. + \cos\gamma\left[1 + (2KC_L)^2\right] - 2KC_L\,(Tw_{MAX} + SwM^2C_{D0} - SwM^2KC_L^2)\right\}. \tag{4-2}$$

On intermediate lift arcs, $\lambda_1$ can be determined from the expression

$$\lambda_1 = \frac{-(1 + \lambda_3 M\cos\gamma + \lambda_4 M\sin\gamma)}{M' + 2KC_L M\gamma'} \tag{4-3}$$

which is obtained by substituting Eq. (4-1) into Eq. (2-5). Thus, the time derivative of $C_L$ on an intermediate lift arc is a function of $\lambda_3$ and $\lambda_4$ (both constants), M, $\gamma$, and $C_L$.

## 2.5 Sequences of Subarcs

From the previous analysis, it is known that a time-optimal path consists of one or more subarcs which appear in Table 1. However, it is not yet known how they may be joined together. The possible sequences of subarcs will now be investigated. Three basic rules are first established.

Corner condition 1: The state variables, Lagrange multipliers, and the Hamiltonian must be continuous at a corner (20).

In addition, each control variable is continuous at a corner if H is regular in that variable (i.e., if H has a unique minimum in that variable, subject to the stated constraints) (21). This result is easily demonstrated, as follows. If z, $\lambda$, $\tau$ and

H are continuous at a corner,

$$H(z, u_+, \lambda, \tau) = H(z, u_-, \lambda, \tau) .$$

Both $u_+$ and $u_-$ must minimize H, if they are optimal controls. Hence H does not have a unique minimum in u, if $u_+ \neq u_-$. For this problem this implies that

Corner condition 2:

Tw can be discontinuous only if $(\lambda_1)_c = 0$, and

$C_L$ can be discontinuous only if either

$$(\lambda_1)_c = (\lambda_2)_c = 0$$

or

$$\frac{(\lambda_2)_c}{2KM(\lambda_1)_c} = C_{L_{AVG}} \text{ and } (\lambda_1)_c > 0 .$$

If $\lambda_1 = \lambda_2 = 0$ at some point, Eqs. (2-1), (2-5) and continuity of $\lambda_3$ and $\lambda_4$ lead to the conclusions that $\lambda_1'$ is continuous and $\lambda_1' = \frac{1}{M} > 0$ at that point. Hence,

Corner condition 3: If $\lambda_1 = \lambda_2 = 0$ at any point on an optimal trajectory, $\lambda_1$ must change from negative to positive at that point.

The first four sections below consider transitions in which Tw does not change, i.e., $\lambda_1$ does not change sign.

2.5.1

$\boxed{I \rightleftarrows II}$ *

*This refers to the transitions between Subarcs I and II of Table 1.

$C_L$ can be discontinuous here only if $(\lambda_1)_c = (\lambda_2)_c = 0$, according to Corner condition 2. Corner condition 3 then implies that $\lambda_1$ changes sign at the corner. According to Table 1, however, $\lambda_1$ must be negative on both subarcs. Hence, $C_L$ must be continuous at this corner, or equivalently, $\lambda_2 = 2KC_{L_{MAX}} M\lambda_1$ at the corner. It follows in addition that $(\lambda_1)_c < 0$, since $(\lambda_1)_c = 0$ implies that $(\lambda_2)_c = 0$ also, which leads to the contradiction noted above. For the transition from I to II, it must also be true that $(C_L')_+ < 0$.

2.5.2

II ⇄ III

The same reasoning as for the transition I ⇄ II leads to the conclusion that $C_L$ is continuous, or equivalently, that $\lambda_2 = 2KC_{L_{MIN}} M\lambda_1$, and $\lambda_1 < 0$ at the corner. For the transition III → II, it must be true that $(C_L')_+ > 0$.

2.5.3

I ⇄ III

A discontinuity in $C_L$, assuming that $C_{L_{MIN}} \neq C_{L_{MAX}}$, requires that $(\lambda_1)_c = (\lambda_2)_c = 0$. Since $\lambda_1 < 0$ on both subarcs, such transitions cannot occur, by Corner condition 3.

2.5.4

IV ⇄ V

From Corner condition 2, a discontinuity in $C_L$ implies that either $\lambda_1 = \lambda_2 = 0$ at the corner, or else $\lambda_2 = 2KC_{L_{AVG}} M\lambda_1$

and $\lambda_1 > 0$ at the corner. Since $\lambda_1$ cannot change sign at the corner, the former case can be ruled out by consideration of Corner condition 3. However, if $\lambda_2 = 2KC_{L_{AVG}} M\lambda_1$ and $\lambda_1 > 0$ at the corner, transitions are possible.

The transitions in which Tw changes will now be investigated. In these transitions $\lambda_1$ must vanish at a corner.

2.5.5

$\boxed{\text{I} \rightarrow \text{IV}}$

Since $\lambda_2 \leq 2KC_{L_{MAX}} M\lambda_1$ and $\lambda_1 < 0$ on Subarc I, and $\lambda_2 \leq 2KC_{L_{AVG}} M\lambda_1$ and $\lambda_1 > 0$ on Subarc IV, $\lambda_1 = 0$ and $\lambda_2 \leq 0$ at a corner.

$\boxed{\text{IV} \rightarrow \text{I}}$

If $\lambda_2 = 0$ at a corner, this transition cannot occur by Corner condition 3. Otherwise, the rules for this transition are the same as for I → IV .

2.5.6

$\boxed{\text{I} \rightarrow \text{V}}$

This transition, which involves a discontinuity in $C_L$ , is possible if $(\lambda_1)_c = (\lambda_2)_c = 0$ , according to Corner conditions 2 and 3.

The transition V → I is not permissible. Corner condition 3 is violated.

2.5.7

$\boxed{\text{III} \rightarrow \text{IV}}$

The same reasoning as for the transition I → V implies that this transition is possible, if $(\lambda_1)_c = (\lambda_2)_c = 0$.

IV → III

Corner condition 3 does not allow this transition.

2.5.8

III ⇄ V

Analysis similar to that in Section 2.5.5 leads to the conditions that

$(\lambda_1)_c = 0 \ , \ (\lambda_2)_c \geq 0$ for III → V

$(\lambda_1)_c = 0 \ , \ (\lambda_2)_c > 0$ for V → III .

2.5.9

II ⇄ IV

$\lambda_1 = 0$ at a corner; consequently $(\lambda_2)_c = 0$ from Eq. (4-1). Hence, Corner condition 3 allows a transition from Subarc II to Subarc IV, but not vice-versa. At this corner, $C_L$ generally will not be continuous. Just before the switch from Subarc II,

$$\lambda_1 \simeq \lambda_1' \ (\tau - \tau_c)$$

$$\lambda_2 \simeq \lambda_2' \ (\tau - \tau_c) \ ,$$

where $\lambda_1' = \frac{1}{M}$ and $\lambda_2' = \lambda_3 M \sin\gamma - \lambda_4 M \cos\gamma$ .

Then,

$$C_L = \frac{\lambda_2}{2KM\lambda_1} \simeq \frac{M}{2K} [\lambda_3 \sin\gamma - \lambda_4 \cos\gamma]$$

immediately before the switch. Hence,

$$C_L \rightarrow \frac{M}{2K} [\lambda_3 \sin\gamma - \lambda_4 \cos\gamma] \qquad (5\text{-}1)$$

as $\tau \rightarrow \tau_c$ from below. In general the right hand side of Eq. (5-1) is not equal to $C_{L_{MAX}}$. Thus, the transition II $\rightarrow$ IV is possible if $(\lambda_1)_c = (\lambda_2)_c = 0$. $C_L$ is generally discontinuous.

2.5.10

II $\rightleftarrows$ V

The transition II $\rightarrow$ V is allowed if $(\lambda_1)_c = (\lambda_2)_c = 0$. $C_L$ is given by Eq. (5-1) immediately before the switch.

The transition V $\rightarrow$ II is not permissible.

The above analysis is summarized in Fig. 3, the diagram of possible sequences of subarcs. Any transition requiring $(\lambda_1)_c = (\lambda_2)_c = 0$ is a relatively unlikely occurrence in which both controls, lift and thrust, change simultaneously. Thus, only the 10 transitions I $\rightleftarrows$ II, II $\rightleftarrows$ III, IV $\rightleftarrows$ V, I $\rightleftarrows$ IV, and III $\rightleftarrows$ V appear to be of real interest. If we let $\lambda_3, \lambda_4 = 0$ (the case in which final range and altitude are not specified), the transitions I $\rightarrow$ V, III $\rightarrow$ IV, II $\rightarrow$ IV, and II $\rightarrow$ V cannot occur, because all $\lambda_i$'s will vanish at the corner, thereby contradicting Eq. (2-5) for the first integral.

Since no terminal constraints on the state have been imposed in the above analysis, any time-optimal maneuver in the vertical plane, not just loop maneuvers, will be composed of these subarcs. In previous work considering minimum time climb performance, the control variable has been taken to be V, $\gamma$ or $\alpha$ (equivalent to $C_L$), while holding the thrust at its maximum level. Optimal solutions consist of paths with $C_L = C_{L_{INT}}$ and $T = T_{MAX}$

(1, 2, 3, 4, 15). In target chasing maneuvers (14), the control is assumed to be $C_L$ or $n$, while using maximum thrust. Minimum time solutions consist of paths with maximum thrust and maximum normal acceleration or maximum lift coefficient.

## 2.6 Analysis of a More Realistic Dynamic Model

In order to obtain the features of a realistic minimum time maneuver, some of the simplifying assumptions made previously shall now be removed. New assumptions are as follows:

1) The atmospheric pressure changes with altitude in the following manner:

$$p = p_o e^{-\varkappa\eta} ,$$

where $p_o$ = pressure at the reference altitude $\eta = 0$. The atmosphere is still isothermal.

2) $C_{D0}$ is a function of Mach number: $C_{D0} = C_{D0}(M)$.

3) $K$ is a function of Mach number: $K = K(M)$.

4) Constraints on normal acceleration due to aircraft structural limits or the pilot's physiological limits are considered.

5) Maximum thrust and minimum thrust are functions of Mach number and altitude:

$Tw_{MAX} = Tw_{MAX}(M, \eta)$ and $Tw_{MIN} = Tw_{MIN}(M,\eta)$.

Generally, the normal acceleration constraint is effective only when the dynamic pressure $(q = \frac{1}{2}\varkappa pM^2)$ is relatively large. The lift coefficient is then bounded above and below by

$$C_{L_X} = \frac{n_{MAX}}{Sw\ e^{-\varkappa\eta} M^2}$$

and

$$C_{L_N} = \frac{n_{MIN}}{Sw\ e^{-\varkappa\eta} M^2} ,$$

respectively. Thus the normal acceleration constraints may be handled as constraints on $C_L$ which depend explicitly on Mach number and altitude. In the relatively low dynamic pressure range, the constant upper and lower bounds on $C_L$ are more restrictive than the state-dependent bounds imposed by the normal acceleration limitation. In the high dynamic pressure range, the reverse is true (see Fig. 4).

2.6.1

Since $C_{L_{MAX}}$, $C_{L_{MIN}}$, $Tw_{MAX}$ and $Tw_{MIN}$ are no longer constant in this case, Eqs. (1-5) and (1-6) will be adjoined to the variational Hamiltonian with the multipliers $\mu_1$ and $\mu_2$:

$$H = \lambda_1 [Tw - Sw\ e^{-\varkappa\eta} M^2 (C_{D0} + KC_L^2) - \sin\gamma]$$
$$+ \frac{\lambda_2}{M} (Sw\ e^{-\varkappa\eta} M^2 C_L - \cos\gamma) + \lambda_3 M\cos\gamma + \lambda_4 M\sin\gamma$$
$$+ \mu_1 (C_L - C_{L_{MAX}}) (C_L - C_{L_{MIN}})$$
$$+ \mu_2 (Tw - Tw_{MAX}) (Tw - Tw_{MIN}) ,$$

where $\mu_1 \geq 0$ , $C_L = C_{L_{MAX}}$ or $C_{L_{MIN}}$

$\mu_1 = 0$ , $C_L = C_{L_{INT}}$

$\mu_2 \geq 0$ , $Tw = Tw_{MAX}$ or $Tw_{MIN}$

$$\mu_2 = 0 \ , \ Tw = Tw_{INT} \ .$$

2.6.2

Necessary conditions of optimality for the problem are

$$M' = Tw - Sw\, e^{-\varkappa\eta}\, M^2 \,(C_{D0} + KC_L{}^2) - \sin\gamma \tag{6-1}$$

$$\gamma' = \frac{1}{M}\,(Sw\, e^{-\varkappa\eta}\, M^2\, C_L - \cos\gamma) \tag{6-2}$$

$$\xi' = M\cos\gamma \tag{6-3}$$

$$\eta' = M\sin\gamma \tag{6-4}$$

$$\begin{aligned}\lambda_1' = {} & \lambda_1 Sw\, e^{-\varkappa\eta}\, M\left[2C_D + M\left(\frac{\partial C_{D0}}{\partial M} + \frac{\partial K}{\partial M}\, C_L{}^2\right)\right] \\ & - \frac{\lambda_2}{M^2}\left(Sw\, e^{-\varkappa\eta}\, M^2 C_L + \cos\gamma\right) - \lambda_3 \cos\gamma - \lambda_4 \sin\gamma \\ & + \mu_1\left[\left(\frac{\partial C_{L_{MAX}}}{\partial M} + \frac{\partial C_{L_{MIN}}}{\partial M}\right) C_L - \left(\frac{\partial C_{L_{MAX}}}{\partial M}\, C_{L_{MIN}}\right.\right. \\ & \left.\left. + \frac{\partial C_{L_{MIN}}}{\partial M}\, C_{L_{MAX}}\right)\right] + \mu_2\left[\left(\frac{\partial Tw_{MAX}}{\partial M} + \frac{\partial Tw_{MIN}}{\partial M}\right) Tw \right. \\ & \left. - \left(\frac{\partial Tw_{MAX}}{\partial M}\, Tw_{MIN} + \frac{\partial Tw_{MIN}}{\partial M}\, Tw_{MAX}\right)\right]\end{aligned} \tag{6-5}$$

$$\lambda_2' = \lambda_1 \cos\gamma - \frac{\lambda_2}{M}\sin\gamma + \lambda_3 M\sin\gamma - \lambda_4 M\cos\gamma \tag{6-6}$$

$$\lambda_3 = \text{const} \tag{6-7}$$

$$\begin{aligned}\lambda_4' = {} & -\lambda_1 Sw\varkappa\, e^{-\varkappa\eta} M^2 C_D + \lambda_2\, Sw\varkappa\, e^{-\varkappa\eta} M\, C_L \\ & + \mu_1\left[\left(\frac{\partial C_{L_{MAX}}}{\partial\eta} + \frac{\partial C_{L_{MIN}}}{\partial\eta}\right) C_L - \left(\frac{\partial C_{L_{MAX}}}{\partial\eta}\, C_{L_{MIN}}\right.\right. \\ & \left.\left. + \frac{\partial C_{L_{MIN}}}{\partial\eta}\, C_{L_{MAX}}\right)\right] + \mu_2\left[\left(\frac{\partial Tw_{MAX}}{\partial\eta} + \frac{\partial Tw_{MIN}}{\partial\eta}\right) Tw\right.\end{aligned}$$

$$- \left( \frac{\partial Tw_{MAX}}{\partial \eta} Tw_{MIN} + \frac{\partial Tw_{MIN}}{\partial \eta} Tw_{MAX} \right) \Big] \qquad (6\text{-}8)$$

$$0 = - \lambda_1 Sw e^{-\varkappa\eta} M^2 2KC_L + \lambda_2 Sw e^{-\varkappa\eta} M$$

$$-\mu_1 \left[ \left( C_{L_{MAX}} + C_{L_{MIN}} \right) - 2 C_L \right] \qquad (6\text{-}9)$$

$$0 = \lambda_1 - \mu_2 \left[ \left( Tw_{MAX} + Tw_{MIN} \right) - 2Tw \right] \qquad (6\text{-}10)$$

$$- \lambda_1 K Sw e^{-\varkappa\eta} M^2 + \mu_1 \geq 0 \qquad (6\text{-}11)$$

$$\mu_1 \geq 0 \text{ for } C_L = C_{L_{MAX}} \text{ or } C_{L_{MIN}} \qquad (6\text{-}12)$$

$$\mu_1 = 0 \text{ for } C_L = C_{L_{INT}} \qquad (6\text{-}13)$$

$$\mu_2 \geq 0 \text{ for } Tw = Tw_{MAX} \text{ or } Tw_{MIN} \qquad (6\text{-}14)$$

$$\mu_2 = 0 \text{ for } Tw = Tw_{INT} \qquad (6\text{-}15)$$

$$\lambda_1 (Tw - Sw e^{-\varkappa\eta} M^2 C_D - \sin\gamma) + \frac{\lambda_2}{M} (Sw e^{-\varkappa\eta} M^2 C_L - \cos\gamma)$$

$$+ \lambda_3 M \cos\gamma + \lambda_4 M \sin\gamma = - 1 \qquad (6\text{-}16)$$

These equations are similar to those for the simpler dynamic model, except that $\lambda_4' \neq 0$, $\mu_1$ and $\mu_2$ enter the $\lambda_1'$ and $\lambda_4'$ equations, and the term $e^{-\varkappa\eta}$ appears in various equations.

### 2.6.3 Characteristics of Subarcs

Investigation will be made of the subarcs corresponding to different control combinations. Eq. (6-10) implies that a subarc with $Tw = Tw_{INT}$ ($\mu_2 = 0$) must have $\lambda_1 \equiv 0$. Consequently

$\lambda_1' \equiv 0$ . This arc is a singular arc, as was observed in the simpler case. If $C_L = C_{L_{INT}}$ $(\mu_1 = 0)$, then $\lambda_2 = 0$, from Eq. (6-9). Then Eqs. (6-5) and (6-16) reduce to

$$0 = -\lambda_3 \cos\gamma - \lambda_4 \sin\gamma$$

$$-1 = \lambda_3 M\cos\gamma + \lambda_4 M\sin\gamma$$

respectively. Inconsistency of these two equations leads to the conclusion that the subarc with $Tw = Tw_{INT}$ and $C_L = C_{L_{INT}}$ does not exist.

For the lift program with $C_L = C_{L_{MAX}}$ $(\mu_1 > 0)$ , with the normal acceleration constraint assumed effective,

$$\mu_1 = -\frac{\lambda_2 \, Sw \, e^{-\varkappa\eta_M}}{(C_{L_{MAX}} - C_{L_{MIN}})} \tag{6-17}$$

from Eq. (6-9). From Eqs. (6-5), (6-16), and (6-17), it then follows that

$$\frac{d}{d\tau}\left(\frac{\partial H}{\partial Tw}\right) = \lambda_1' = \frac{1}{M}\left(1 - \frac{2\lambda_2 \cos\gamma}{M}\right) - \lambda_2 Sw\, e^{-\varkappa\eta_M}\left(\frac{\partial C_{L_{MAX}}}{\partial M}\right) = 0 ,$$

or

$$\lambda_2 = \frac{-M}{2(n_{MAX} - \cos\gamma)} , \tag{6-18}$$

where use has been made of the relation

$$C_{L_{MAX}} = \frac{n_{MAX}}{Sw\, e^{-\varkappa\eta_M}\, 2} . \tag{6-19}$$

Furthermore,

$$\frac{d^2}{d\tau^2}\left(\frac{\partial H}{\partial Tw}\right) = \lambda_1'' = \left[\frac{1}{M^3}(4\lambda_2 \cos\gamma - M) - \lambda_2 Sw\, e^{-\varkappa\eta}\left(\frac{\partial C_{L_{MAX}}}{\partial M} + M\frac{\partial^2 C_{L_{MAX}}}{\partial M^2}\right)\right] Tw$$

+ other terms not involving $Tw$ .

The generalized Legendre-Clebsch condition requires that

$$\frac{\partial}{\partial Tw}\left[\frac{d^2}{d\tau^2}\left(\frac{\partial H}{\partial Tw}\right)\right] = \frac{1}{M^3}(4\lambda_2\cos\gamma - M) - \lambda_2 Sw\, e^{-\varkappa\eta}\frac{\partial C_{L_{MAX}}}{\partial M} - \lambda_2 Sw\, e^{-\varkappa\eta} M \frac{\partial^2 C_{L_{MAX}}}{\partial M^2} \leq 0 \quad .$$

Substituting Eq. (6-18), and $\frac{\partial C_{L_{MAX}}}{\partial M}$ and $\frac{\partial^2 C_{L_{MAX}}}{\partial M^2}$ derived from Eq. (6-19) into above equation, we have

$$\frac{1}{M^2} \leq 0 \quad .$$

Since $M$ must be real, the generalized Legendre-Clebsch condition is not satisfied. Hence, an arc with $Tw_{INT}$ and $C_{L_{MAX}}$ is not optimal. The same result will hold for the lift program with $C_L = C_{L_{MIN}}$. For the case in which $C_L = C_{L_{MAX}}$ or $C_{L_{MIN}}$ without the normal acceleration constraint, the same analysis as for the simpler case is applicable, since the term involving $\mu_1$ vanishes in Eq. (6-5). Thus, intermediate thrust arcs are not optimal in the more realistic case, just as in the simpler case.

For an arc with $Tw = Tw_{MAX}$ ($\mu_2 > 0$), we have $\lambda_1 < 0$ from Eq. (6-10). Then, from Eq. (6-9)

$$\frac{\lambda_2}{2KM\lambda_1} \geq C_{L_{MAX}} \Longrightarrow C_L = C_{L_{MAX}}$$

$$C_{L_{MIN}} < \frac{\lambda_2}{2KM\lambda_1} < C_{L_{MAX}} \Longrightarrow C_L = C_{L_{INT}} = \frac{\lambda_2}{2KM\lambda_1}$$

$$\frac{\lambda_2}{2KM\lambda_1} \leq C_{L_{MIN}} \Longrightarrow C_L = C_{L_{MIN}} .$$

For an arc with $Tw = Tw_{MIN}$ $(\mu_2 > 0)$, we have $\lambda_1 > 0$. For intermediate lift, we have $\lambda_1 \leq 0$ from Eq. (6-11). This result contradicts the above conclusion concerning $\lambda_1$. Hence a subarc with $Tw = Tw_{MIN}$ and $C_L = C_{L_{INT}}$ cannot be an optimal arc. For $C_L = C_{L_{MAX}}$ $(\mu_1 > 0)$ or $C_L = C_{L_{MIN}}$ $(\mu_1 > 0)$, we can infer that

$$\frac{\lambda_2}{2KM\lambda_1} \begin{cases} < \dfrac{C_{L_{MAX}} + C_{L_{MIN}}}{2} \triangleq C_{L_{AVG}} \Longrightarrow C_L = C_{L_{MAX}} \\ > C_{L_{AVG}} \Longrightarrow C_L = C_{L_{MIN}} \end{cases}$$

as in the simpler case.

An arc with $Tw = Tw_{MAX}$ $(\mu_2 = 0)$ or $Tw_{MIN}$ $(\mu_2 = 0)$, or $C_L = C_{L_{MAX}}$ $(\mu_1 = 0)$ or $C_{L_{MIN}}$ $(\mu_1 = 0)$ leads to contradiction between Eq. s (6-5) and (6-16) except possibly at isolated points.

These results are similar to the simplified ones. Hence, the transition between subarcs are analogous to those for the simplified case. However, there are two types of $C_{L_{MAX}}$ subarcs - those for which $C_{L_{MAX}}$ is constant and those for which $C_{L_{MAX}}$ depends on the state, as shown in Fig. 4. There are similarly

two types of $C_{L_{MIN}}$ subarcs.

2.6.4

The time derivative of the lift coefficient on intermediate lift arcs is given by

$$C_L' = \frac{1}{2KM}\left\{\frac{M}{\lambda_1}\left[\lambda_3(\sin\gamma + 2KC_L\cos\gamma) - \lambda_4(\cos\gamma - 2KC_L\sin\gamma)\right]\right.$$

$$+ \cos\gamma\left[1 + (2KC_L)^2\right]$$

$$- 2KC_L\left[(Tw_{MAX} - Sw\, e^{-\kappa\eta} M^2 KC_L{}^2)\left(1 + \frac{K}{M}\frac{\partial K}{\partial M}\right)\right.$$

$$+ Sw\, e^{-\kappa\eta} M^2 C_{D0}\left(1 - \frac{K}{M}\frac{\partial K}{\partial M}\right) - \frac{K}{M}\frac{\partial K}{\partial M}\sin\gamma$$

$$\left.\left. + Sw\, e^{-\kappa\eta} M^3\left(\frac{\partial C_{D0}}{\partial M} + \frac{\partial K}{\partial M} C_L{}^2\right) - M\frac{\partial Tw_{MAX}}{\partial M}\right]\right\} ,$$

where $\lambda_1 = \dfrac{-(1 + \lambda_3 M\cos\gamma + \lambda_4 M\sin\gamma)}{M' + 2KMC_L\gamma'}$ .

# III. NUMERICAL METHODS

## 3.1 Simpler Case

The optimization problem under consideration here is expressible as a two-point boundary value problem. Differential equations (1-1), (1-2), (1-3), (1-4), (2-1), (2-2), (2-3), and (2-4) must be satisfied, subject to mixed boundary conditions, with the optimal control along the trajectory determined by the state variables and Lagrange multipliers, as described in Part II. The initial time and the initial state are given, but the initial Lagrange multipliers and the terminal time are unknown. These five unknown parameters must be determined such that the following terminal conditions are satisfied:

$$M_f \quad \text{specified} \quad \text{or} \quad (\lambda_1)_f = 0 \tag{7-1}$$

$$\xi_f \quad \text{specified} \quad \text{or} \quad (\lambda_3)_f = 0 \tag{7-2}$$

$$\eta_f \quad \text{specified} \quad \text{or} \quad (\lambda_4)_f = 0 \tag{7-3}$$

$$\gamma_f = 2\pi \tag{7-4}$$

$$H_f = -1 \tag{7-5}$$

Since this two-point boundary value problem does not appear to have an analytical solution, some form of numerical optimization technique must be employed. A shooting (or neighboring extremal) method was used. The basis of such a method, as applied to this problem, is as follows. By making use of the fact that $\lambda_3$ and $\lambda_4$ are constant and $H(\tau) = -1$ an extremal trajectory may be generated by guessing the three quantities $(\lambda_1)_i$, $\lambda_3$ and $\lambda_4$, and integrating differential equations for

M, $\gamma$, $\xi$, $\eta$, and $\lambda_1$ forward, subject to the required initial conditions on the state variables. The optimal control along the trajectory is determined in terms of the state variables and Lagrange multipliers, as described in Part II. $\lambda_2(\tau)$ is determined from the condition that $H(\tau) \equiv -1$. The final time $\tau_f$ is chosen to be the time at which $\gamma(\tau) = 2\pi$. In general, the guessed values of the parameters $(\lambda_1)_i$, $\lambda_3$, and $\lambda_4$ will not be such that terminal conditions (7-1), (7-2), and (7-3) are satisfied. A three-dimensional search must then be made for the set of initial parameters which causes the required terminal conditions to be satisfied.

If $\xi_f$ and $\eta_f$ are both specified, a full three-dimensional search is required. If $\xi_f$ is specified but $\eta_f$ is not, the search is two-dimensional since $\lambda_4 \equiv 0$. The situation is analogous if $\eta_f$ is specified, but $\xi_f$ is not. If neither $\xi_f$ nor $\eta_f$ is specified, the search is one-dimensional - $(\lambda_1)_i$ must be chosen such that Eq. (7-1) is satisfied.

On intermediate lift arcs, it is more convenient to integrate Eq. (4-2) for $C_L$ than Eq. (2-1) for $\lambda_1$. On such arcs, $\lambda_1$ and $\lambda_2$ are determined according to Eqs. (4-1) and (4-3).

Numerical integration with a fourth-order Runge-Kutta method was carried out. About five hundred steps of integration were shown to be sufficient for securing four digit accuracy at the final point, by comparing the computed results for various step sizes. Corner conditions for other subarcs, described in Fig. 3, may also be monitored along with trajectory computation. Since

a corner is not necessarily located at a discrete point of integration, its location is determined by linear interpolation between two successive points between which a corner is determined to exist.

Several other parameters can be considered as variable besides those which we have already considered, for example, the weight and wing area of the aircraft and its initial speed and altitude. The hypothetical set of data describing the aircraft, atmospheric conditions and gravity given in Table 2 were used. The aircraft data are approximately those of the fighter-trainer aircraft XT-2 of Japan. An initial speed of Mach 0.9 is assumed.

3.1.1 $M_f$, $\xi_f$ and $\eta_f$ are not specified.

A one-dimensional search for $(\lambda_1)_f = 0$ will be used. Since it is not known a priori what combination of subarcs will produce an optimal solution, exploratory computations for a minimum time path were made for the case $C_{L_{MAX}} = 1.0$ and $Tw_{MAX} = 0.5$. Paths with several combinations of subarcs, for example, I, I-II-I, or IV-I etc., were computed and the performance indices of the maneuvers were compared. From these results, it is expected that the control program for a time optimal path does not deviate much from that of a path with $C_{L_{MAX}}$ and $Tw_{MAX}$. This conclusion is confirmed by private talks with several pilots. The standard procedure is to pull the control stick back to develop lift force from level or diving flight, with maximum thrust. After the normal acceleration reaches its upper limit (4 ~ 5 g's is the physiological limit) they maintain

this limit until the maximum lift coefficient is less than the normal acceleration limit, due to a decrease in dynamic pressure. This description is for a fighter aircraft with $C_{L_{MAX}} \sim 1$ and $Tw_{MAX} \sim 0.5$, at an entry speed of roughly Mach 0.9. This suggests how we might make an initial guess for the one-dimensional search.

An initial $(C_{L_{INT}}, Tw_{MAX})$ arc can be generated by integration of Eqs. (1-1), (1-2), (1-3), (1-4), and (4-2), subject to given initial conditions of state variables, by guessing the initial value of $C_L$.

Once $C_L$ has reached $C_{L_{MAX}}$, assuming that $\lambda_1 < 0$ at that point, Subarc I will follow, according to the corner conditions for the transition $II \rightarrow I$. On Subarc I, Eq. (2-1) for $\lambda_1$ should be integrated from the corner, rather than the $C_L'$ equation, which holds only on intermediate lift arcs. Integration to the final point, at which $\gamma_f = 2\pi$, yields the final value of $\lambda_1$, together with $\lambda_2$ and other state variables. Since this value of $(\lambda_1)_f$ is determined by the guessed value of $(C_L)_i$, we can determine the $(C_L)_i$ for which $(\lambda_1)_f = 0$ by varying $(C_L)_i$. The control programs and the corresponding flight path are obtained at the same time. For the case with $C_{L_{MAX}} = 1.0$ and $Tw_{MAX} = 0.5$, the optimal path has been found and is shown in Fig. 8-a. Only one stationary solution was found in this case. The control programs along this trajectory are consistent with the results of the exploratory computations and the standard pilots' procedure.

The initial value of $C_L$ for an optimal solution changes if $C_{L_{MAX}}$ and $Tw_{MAX}$ are changed. If either $C_{L_{MAX}}$ or $Tw_{MAX}$ is decreased, while holding the other constant, $(C_L)_i$ eventually reaches $C_{L_{MAX}}$. Below that value of $C_{L_{MAX}}$ or $Tw_{MAX}$, a $(C_{L_{INT}}, Tw_{MAX})$ arc cannot exist at $\tau = 0$. Hence, a $(C_{L_{MAX}}, Tw_{MAX})$ arc will be the initial part of an optimal path. For such a path the initial value of $\lambda_1$ can be varied so as to obtain $(\lambda_1)_f = 0$.

Following the above procedure, corner conditions for other subarcs may appear in the middle of the path; e.g., $\lambda_1 = 0$ for $Tw = Tw_{MIN}$, $\dot{\lambda}_1 = 2KC_L M\lambda_1$ for $C_L = C_{L_{INT}}$, and so forth. In these cases, computation should also be made of paths with other subarcs, and the performance indices compared.

Through this process, the time optimal solution for each combination of $C_{L_{MAX}}$ and $Tw_{MAX}$ can be obtained. The results are plotted in Fig. 8-b to Fig. 8-i.

For the case in which $M_f$ is specified, a one-dimensional search can be applied to choose $(C_L)_i$ or $(\lambda_1)_i$ so as to produce the specified value of $M_f$.

3.1.2 $M_f$ and $\eta_f$ are not specified, and $\xi_f$ is specified.

The dimension of the search process is now increased to two. Since we have already obtained the optimal solution for the case in which $M_f$, $\xi_f$, and $\eta_f$ are not specified, this solution may be used as an initial guess for the two-dimensional search.

Varying $(C_L)_i$ or $(\lambda_1)_i$ from the corresponding values of

the optimal solution of Section 3.1.1, while holding $\lambda_3 = 0$ and $\lambda_4 = 0$, produces changes in $(\lambda_1)_f$ and $\xi_f$. Varying $\lambda_3$, while holding $(C_L)_i$ or $(\lambda_1)_i$ the same as in the optimal solution of Section 3.1.1, and maintaining $\lambda_4 = 0$, also changes $(\lambda_1)_f$ and $\xi_f$. From these results, we can construct the following Jacobian matrix (or transition matrix) by numerical differentiation of $(\lambda_1)_f$ and $\xi_f$ with respect to $(C_L)_i$ or $(\lambda_1)_i$ and $\lambda_3$.

$$\frac{\partial [(\lambda_1)_f,\ \xi_f]}{\partial [(C_L)_i \text{ or } (\lambda_1)_i,\ \lambda_3]} \quad .$$

If the resulting values of $(\lambda_1)_f$ and $\xi_f$ are sufficiently close to their desired values, an optimal solution can be obtained with reasonable accuracy by an iterative process using the inverse of the above matrix.

For the case in which $M_f$ is specified, a similar technique used above can be applied by replacing $(\lambda_1)_f$ with $M_f$. If $\eta_f$ is specified and $\xi_f$ is not specified, the same procedure is valid if $\lambda_4$ and $\eta_f$ are used in place of $\lambda_3$ and $\xi_f$.

3.1.3 $M_f$ is not specified, $\xi_f$ and $\eta_f$ are both specified.

In this case it is possible to use the optimal solutions of Sections 3.1.1 or 3.1.2, as an initial guess for the required three-dimensional search. This leads to the use of a three-dimensional Jacobian matrix

$$\frac{\partial [(\lambda_1)_f,\ \xi_f,\ \eta_f]}{\partial [(C_L)_i \text{ or } (\lambda_1)_i,\ \lambda_3,\ \lambda_4]} \quad .$$

This technique can also be applied to the case in which $M_f$ is specified, simply by replacing $(\lambda_1)_f$ with $M_f$.

## 3.2 More Realistic Case

A more realistic case introduces not only aerodynamic parameters which vary with Mach number, but also a more realistic atmosphere which includes the variation of pressure with altitude. In this case, $\lambda_4$ is no longer constant, because of Eq. (6-8). Hence, one additional differential equation for $\lambda_4$ should be integrated along with the five other differential equations. Two cases need to be considered.

### 3.2.1 Without Normal Acceleration Constraint

#### 3.2.1.1 $M_f$, $\xi_f$ and $\eta_f$ are not specified

This case corresponds to the case in Section 3.1.1. However, a two-dimensional search for the values of $(C_L)_i$ or $(\lambda_1)_i$, and $(\lambda_4)_i$ which produce $(\lambda_1)_f = 0$ and $(\lambda_4)_f = 0$ is necessary. A starting solution with values of $(\lambda_1)_f$ and $(\lambda_4)_f$ reasonably close to zero can be obtained by making several trial computations with various values of $(C_L)_i$ or $(\lambda_1)_i$ and $(\lambda_4)_i$. Starting from this nominal solution, an optimal solution can be computed using a two-dimensional Jacobian matrix

$$\frac{\partial \left[ (\lambda_1)_f,\ (\lambda_4)_f \right]}{\partial \left[ (C_L)_i \text{ or } (\lambda_1)_i,\ (\lambda_4)_i \right]} ,$$

obtained by varying $(C_L)_i$ or $(\lambda_1)_i$ and $(\lambda_4)_i$ about the nominal solution.

For the case in which $M_f$ and/or $\eta_f$ are specified, $M_f$

and/or $\eta_f$ are used in place of $(\lambda_1)_f$ and/or $(\lambda_4)_f$ respectively.

3.2.1.2 $M_f$ and $\eta_f$ are not specified, and $\xi_f$ is specified.

In this case, a neighboring extremal technique can be applied starting from the optimal solution of Section 3.2.1.1, using the three-dimensional Jacobian matrix

$$\frac{\partial \left[(\lambda_1)_f,\ \xi_f,\ (\lambda_4)_f\right]}{\partial \left[(C_L)_i \text{ or } (\lambda_1)_i,\ \lambda_3,\ (\lambda_4)_i\right]}$$

For the case in which $M_f$ and/or $\eta_f$ are specified, it is necessary to replace $(\lambda_1)_f$ and/or $(\lambda_4)_f$ with $M_f$ and/or $\eta_f$ respectively.

3.2.2 With Normal Acceleration Constraint

In this case, $C_L$ is sometimes limited by the $n_{MAX}$ constraint. Where $C_{L_{MAX}}$ appears in state equations and Euler-Lagrange equations, it should be expressed in terms of $n_{MAX}$, M and $\eta$. A corner to this arc from other arcs will be a point where n becomes equal to $n_{MAX}$. Since the $n_{MAX}$ constraint appears in the relatively high dynamic pressure range and the dynamic pressure normally decreases rapidly during a loop maneuver, this constraint is effective mainly on the initial part of a flight path.

3.2.2.1 $M_f$, $\xi_f$ and $\eta_f$ are not specified.

During the search process for $(\lambda_1)_f = 0$ and $(\lambda_4)_f = 0$, if $(C_L)_i$ is not affected by the $n_{MAX}$ constraint, i.e.,

$(C_L)_i < C_{L_X}$, the procedure in Section 3.2.1 is also applicable. If $(C_L)_i$ is constrained by $n_{MAX}$, the maneuver should start with $C_L = C_{L_X}$. In this case, the initial arc is considered to be with $C_{L_{MAX}}$ constrained by $n_{MAX}$. Hence, a Jacobian matrix

$$\frac{\partial[(\lambda_1)_f, (\lambda_4)_f]}{\partial[(\lambda_1)_i, (\lambda_4)_i]}$$

should be applied to obtain the solution, as was done for an initial arc of $(C_{L_{MAX}}, Tw_{MAX})$.

For cases with different boundary conditions, a technique similar to that described in Sections 3.2.1.1 and 3.2.1.2 can be applied.

# IV. RESULTS AND DISCUSSION

Numerical computations have been made in several cases, based on the theoretical work and numerical methods discussed above. The effects of the maximum lift coefficient and thrust on the control program have been obtained for the case in which final speed, altitude and range are not specified. Trajectories with different terminal boundary conditions have been investigated for the particular case of $C_{L_{MAX}} = 1.0$ and $Tw_{MAX} = 0.5$. The more realistic model also has been examined for the same parameter values.

## 4.1 Simpler Case

### 4.1.1 $M_f$, $\xi_f$ and $\eta_f$ are not specified.

The general effects of the magnitudes of $C_{L_{MAX}}$ and $Tw_{MAX}$ on the control program are shown in Fig. 7. (About one hundred points in the $Tw_{MAX}$ vs. $C_{L_{MAX}}$ plane were investigated.) The $Tw_{MAX}$ vs. $C_{L_{MAX}}$ plane may be divided into distinct regions corresponding to different types of control histories. The boundary line labeled "$C_{L_{INT}}$ Initially" indicates that the $C_L$ program begins with a $C_{L_{INT}}$ arc, in the region to the right of that line. The label "$C_{L_{INT}}$ In The Middle" indicates that the $C_L$ program has a $C_{L_{INT}}$ arc in its middle part, in the region of the plane below that line. The line labeled "$Tw_{MIN}$ In The Middle" divides the plane of $Tw_{MAX}$ vs. $C_{L_{MAX}}$ according to whether or not $Tw = Tw_{MIN}$ in the middle. The label "$Tw_{MIN}$ Initially" indicates that the Tw program begins with the $Tw_{MIN}$ arc, in the region to the left of that line.

The regions determined by these boundary lines are denoted by the letters A to K, corresponding to the optimal $C_L$ and $T_w$ programs shown in the upper part of the figure, except for regions J and K. For J, no stationary solutions have been found, although the maneuver can be completed. For K, no control programs are plotted, since the maneuver cannot be completed. Representative histories of the control and state variables and Lagrange multipliers for each region are shown in Figs. 8-a to 8-j. The regions C, D, G, and I have a second stationary solution, without the $C_{L_{INT}}$ arc in the middle of the path, except for the region below the broken line, in which only one locally optimal path exists. However, these paths produce larger minimum times than those shown in Fig. 7.

The boundaries separating regions B, E and F have other characteristics which are shown in Fig. 9. In the neighborhood of the boundary line between points 1 to 2 (separating regions B and F), there are three locally optimal solutions of types B, E and F, which have different values of maneuver time. In region B, the time for solution type B is shortest among the three possibilities, and in region F, the time for solution type F is shortest. The minimum time solution switches from one type of solution to the other across the boundary line 1-2, in Fig. 9. This phenomenon can be explained in terms of Fig. 10. $(\lambda_1)_f$ and $t_f$ are plotted versus $(\lambda_1)_i$ for three cases with different $Tw_{MAX}$, but the same $C_{L_{MAX}}$. The smallest value, the intermediate value, and the largest value of $(\lambda_1)_i$ which give $(\lambda_1)_f = 0$ represent type B, E

and F solutions, respectively. The solution giving the smallest value of $t_f$ switches from type B to F as $Tw_{MAX}$ decreases. The type E solution results in a larger $t_f$ than occurs in the other cases. Similar solution switchings have been observed across the boundary lines 2-3 and 2-5. Across the boundary lines 3-4 and 5-6, the solution changes from one type to the other continuously. It is expected that there are three locally optimal solutions with different kinds of thrust programs, which give the same value of maneuver time at the point 2 in Fig. 9.

It can be inferred that optimal paths in the regions to the left of regions I and F begin with a $Tw_{MIN}$ arc, which corresponds to positive $\lambda_1$. The time histories of $\lambda_1$ in this region ($C_{L_{MAX}} < 0.68$) show that the duration of the $Tw_{MIN}$ arc is so long that the flight path angle cannot be increased past $90^o$. This means that the aircraft cannot complete a loop maneuver, and hence, type F or I paths cannot exist. When $Tw_{MAX}$ is somewhat larger, it is possible to have a solution of type B giving $(\lambda_1)_f = 0$ (Region B at upper-left corner in Fig. 7); however, decreasing $Tw_{MAX}$ while holding $C_{L_{MAX}}$ constant, or decreasing $C_{L_{MAX}}$ while holding $Tw_{MAX}$ constant in the medium $Tw_{MAX}$ region, results in paths of type B which fail to give $(\lambda_1)_f = 0$ (Region J), as seen in Fig. 11. For the case $C_{L_{MAX}} = 0.6$ and $Tw_{MAX} = 0.3$, the control programs for minimum time paths have been investigated. The flight path and Lagrange multiplier data are shown in Fig. 8-j for a path beginning with ($C_{L_{MAX}}$, $Tw_{MAX}$). This path does not yield $(\lambda_1)_f = 0$. No stationary solutions have been found for

trajectories beginning with other control programs, either.

Region K denotes that the aircraft cannot complete the maneuver, because the flight path angle cannot be increased beyond $90^{o}$, due to thrust, weight and drag balance, even using maximum thrust.

Modifications in the control history map (Fig. 7) can be expected if the initial conditions are changed.

Contours of minimum maneuver time are plotted in the plane of $Tw_{MAX}$ vs. $C_{L_{MAX}}$ in Fig. 12. The higher values of $Tw_{MAX}$ and $C_{L_{MAX}}$ give shorter maneuver times. Contours of final speed for minimum time maneuvers also plotted in Fig. 13, revealing a different trend with $C_{L_{MAX}}$. This can be expected from the role of $C_L$ in the drag equation. The range at the final point (the horizontal distance of the final point from the starting point) behaves similarly to the maneuver time, as shown in Fig. 12. This may be easily observed from the flight path data given in Figs. 8-a to 8-i. The final altitude does not vary as strongly as other variables. From these results it is concluded that large thrust is desirable for shorter maneuver time and higher final speed.

From the viewpoint of inlet, duct and engine design, the control histories of lift and thrust shown in Figs. 8-a to 8-i present a severe design requirement. Maximum thrust at a high angle of attack and low speed is required for a minimum time maneuver. This will produce much distortion in inlet and duct air flow and may induce compressor stall of the engine. Furthermore, investigation of the transient effect of abrupt thrust level

changes on the inlet and duct air flow and the engine performance will be required, especially at low speeds, as occurs in the regions of medium and low $Tw_{MAX}$ in Figs. 8-e to 8-i.

4.1.2 $M_f$ and $\eta_f$ are not specified, and $\xi_f$ is specified.

The effect of $\lambda_3$ on the final range has been studied for the case $C_{L_{MAX}} = 1.0$ and $Tw_{MAX} = 0.5$. $\lambda_3$ and $(C_L)_i$ were varied so as to produce changes in the final range, with $(\lambda_1)_f = 0$. The control programs and the final ranges corresponding to various choices of $\lambda_3$ have been obtained. These trajectories are optimal loops with specified final ranges. The result for the case $(C_L)_i = 0.4$ is shown in Fig. 14. From this it is observed that the final range increases by about 1,300 ft. and the final altitude changes from negative to positive, if the initial $C_L$ is decreased by about 0.5. Trajectories beginning with $(C_{L_{MAX}}, Tw_{MAX})$ have also been considered. $\lambda_3$ and $(\lambda_1)_i$ are varied such that the final range changes and $(\lambda_1)_f$ remains zero. Fig. 15 shows that the control histories are different and that the final range increases drastically relative to the result in Fig. 8-a, even though both cases have the same combination of $C_{L_{MAX}}$ and $Tw_{MAX}$.

Among seven trials with different values of $\lambda_3$, the case $C_{L_{MAX}} = 1.0$ and $Tw_{MAX} = 0.5$ was found to have the minimum $x_f$ of 4,384 ft., using the constant control $C_L = C_{L_{MAX}}$ and $Tw = Tw_{MAX}$. Smaller values of $x_f$ would require a more extensive exploration of control programs.

4.1.3 $M_f$ is not specified, $\xi_f$ and $\eta_f$ are specified.

Although this case is normally solved by means of a three-dimensional search, it is possible to use a two-dimensional search if only two final values are of interest. For the case with $C_{L_{MAX}} = 1.0$ and $Tw_{MAX} = 0.5$, the optimal solution, for which $(\lambda_1)_f = 0$ and $\eta_f = 0$, has been obtained by suitably varying $\lambda_3$ and $\lambda_4$ from the result of Fig. 14, while holding $(C_L)_i = 0.4$. This is shown in Fig. 16. The trajectory shown is thus optimal for the final range so determined.

4.2 More Realistic Case

4.2.1 Without Normal Acceleration Constraint

The case which takes into account changes in pressure with altitude, the effects of altitude and Mach number on thrust, and changes in $C_{D0}$ and $K$ as functions of Mach number has been computed on the path $C_{L_{MAX}} = 1.0$ and $(Tw_{MAX})_i = 0.5$, with $\lambda_3 = 0$ and $(\lambda_4)_f = 0$. There is not much difference between the control history in this case and the simpler case, as may be seen by comparing Figs. 17 and 8-a. The time for maneuver, the altitude at the top of the loop, and the final range are larger in the former than in the latter. Since the effects of altitude and Mach number on the control history are relatively small, the simpler case is a reasonable approximation to the more realistic situtation.

4.2.2 With Normal Acceleration Constraint

The normal acceleration constraint is now added to the

problem treated in Section 4.2.1. In this case, an arc of $C_{L_{MAX}}$ subject to the $n_{MAX}$ constraint replaces the $C_{L_{INT}}$ arc. It is followed by an arc of $C_{L_{MAX}}$ without the $n_{MAX}$ constraint, as shown in Fig. 18. Although the initial program has changed from $C_{L_{INT}}$ to $C_{L_{MAX}}$, the similarity in the numerical values of $C_L$ does not cause the values of maneuver time and the terminal state variables to change appreciably relative to the results of Section 4.2.1. In this example, the $n_{MAX}$ constraint has its major effect on the initial part of the path, since the initial dynamic pressure is large. The effect of the constraint decreases with an increase in the value of $n_{MAX}$ (see Fig. 19). If $n_{MAX}$ is taken to be 7.33, the structural limit load factor for fighter aircraft (22), most of the control history map need not be modified. When $n_{MAX}$ is decreased to 5, major changes must be made, especially in the initial part of the path. However, the dynamic pressure decreases as the maneuver progresses, so that the $n_{MAX}$ constraint soon becomes ineffective. Hence, the effect of the $n_{MAX}$ constraint depends upon how long the constraint is effective relative to the overall maneuver time. In the above example, the duration of 5g normal acceleration is about 5 seconds, compared with $t_f = 48$ seconds.

# V. CONCLUSION

Minimum time loop maneuvers of high performance jet aircraft have been investigated through the calculus of variations. Numerical computations for time optimal paths have been made for a hypothetical aircraft at an initial altitude of 20,000 ft. and a speed of Mach 0.9. From the theoretical analysis and numerical results, the following conclusions have been derived.

There are several types of subarcs which may be joined together to form an optimal path. There are no subarcs with $Tw_{INT}$, or $C_{L_{INT}}$ and $Tw_{MIN}$. The optimal control is uniquely determined by the state variables and Lagrange multipliers. Possible transitions between optimal subarcs have been established by applying the corner conditions of variational calculus. These results are applicable to any minimum time maneuver in the vertical plane.

For the given initial conditions, the effects of the magnitudes of $C_{L_{MAX}}$ and $Tw_{MAX}$ on the control program have been plotted in the control history map, for the case in which final speed, range and altitude are not specified. The $Tw_{MAX}$ vs. $C_{L_{MAX}}$ plane has been divided into eleven regions. Nine of these regions are characterized by qualitatively different control programs for minimum time paths. One of the remaining two has admissible solutions; however, no stationary solutions have been found yet. In the other region the maneuver cannot be completed. The flight path angle cannot increase beyond $90^{o}$, due to the balance of thrust, weight and drag. These features are observed in the low $C_{L_{MAX}}$

region. In the region of low $C_{L_{MAX}}$ and medium $Tw_{MAX}$, it was observed that there were three locally optimal solutions which have different thrust programs.

In the relatively high $C_{L_{MAX}}$ and high $Tw_{MAX}$ region, a path is varied mainly by means of lift control rather than thrust. In the relatively low $C_{L_{MAX}}$ and low $Tw_{MAX}$ region, both lift and thrust are important control variables.

The effects of the magnitudes of $C_{L_{MAX}}$ and $Tw_{MAX}$ on the time and the final range of the minimum time maneuver are similar. Larger values of $C_{L_{MAX}}$ and $Tw_{MAX}$ give shorter time and smaller range. The effects of $C_{L_{MAX}}$ and $Tw_{MAX}$ on the final speed are different, however. To increase the speed at the end of a minimum time maneuver, an increase in $Tw_{MAX}$ or a decrease in $C_{L_{MAX}}$ is favorable. Final altitude is affected relatively little by these quantities.

The maximum thrust required at a high angle of attack and low speed, around the top of the loop maneuver, will impose severe restrictions on the inlet, duct and engine design, from the standpoint of compressor stall of the engine. If $C_{L_{MAX}}$ is relatively small and $Tw_{MAX}$ is medium, investigation of the dynamic behavior of the air flow in the inlet and duct may be necessary, since the thrust changes abruptly from its minimum to its maximum level.

The simplifying assumptions made on the altitude, pressure and Mach number changes have been found not to have a major effect on the control program and aircraft performance. Hence,

this approach is considered to be good enough to obtain the general features and characteristics of this problem.

Under the assumed initial conditions, the normal acceleration constraint exerts its main influence on the initial part of the maneuver, just as though a $C_{L_{INT}}$ arc were inserted. Usually the speed of the aircraft decreases in the early stage of the maneuver, and the aircraft soon attains its $C_{L_{MAX}}$. Since $C_L = C_{L_{MAX}}$ along most of the trajectory, the significance of the $n_{MAX}$ arc is heavily dependent upon the ratio of the magnitudes of $n_{MAX}$ and $C_{L_{MAX}}$, if the initial dynamic pressure is held fixed.

Since the control history map has been obtained for a particular combination of values of wing loading, initial altitude and initial speed, the pattern of the map may be affected by changes in these parameters. These changes may be easily obtained by the numerical methods used in this thesis.

There are several additional performance optimization problems in which pilots and designers are interested. These include problems of the energy height difference maximization ($he = y + \frac{V^2}{2g}$, see Appendix B), fuel consumption minimization, and the target pursuit problem, the latter being a differential game problem.

# APPENDIX A

## The Effect of Transient Motion

In this thesis, the equations of motion are established based upon the assumption that the aircraft is a point mass. The angular momentum balance around the center of gravity is neglected. As long as the control history of $C_L$ is smooth, i.e., its time derivative is continuous, this assumption is appropriate. At the corner point between two subarcs with intermediate $C_L$ and maximum $C_L$, for example, the time derivative of $C_L$ is usually not continuous.

Angular equilibrium then causes a transient pitching motion and, consequently, a deviation from the nominal path around the corner. However, since the duration of this transient motion is relatively short compared with the controlled subarcs, the effect of transient motion on the overall maneuver can be neglected if control changes are not frequent.

# APPENDIX B

## Maximization Problem of Energy Height Difference

The performance index to be minimized is given in the following form:

$$I = [G\ (t, z)]_i^f$$

$$= (\eta_i - \eta_f) + \frac{1}{2}\ (M_i^2 - M_f^2)\ .$$

If we assume that the differential constraints and inequality control constraints are the same as in Part II, Eqs. (1-1) to (2-4) except Eq. (1-7) are also applicable, and the first integral becomes

$$\lambda_1\ (Tw - SwM^2 C_D - \sin\gamma) + \frac{\lambda_2}{M}\ (SwM^2\ C_L - \cos\gamma)$$

$$+ \lambda_3\ M\cos\gamma + \lambda_4\ M\sin\gamma = H = \text{constant}\ .$$

If all the initial and final conditions are given except the speed, range and altitude at the final point, the transversality conditions give

$$(\lambda_1)_f = -M_f\ ,\ (\lambda_3)_f = 0\ ,\ (\lambda_4)_f = -\ 1\ .$$

The possible subarcs and their relationships to the Lagrange multipliers are the same as in the time-optimal problem.

To solve this problem it is necessary to establish the sequence diagram of subarcs. One additional unknown parameter enters the problem since $H$ is not known. The transition routes between subarcs which require that $\lambda_1 = \lambda_2 = 0$ will change their direction if $H > 0$ .

## REFERENCES


1. Miele, A., and Capellari, J. O., Jr., "Approximate Solutions to Optimum Flight Path Trajectories for a Turbojet-Powered Aircraft," NASA TN-152 (1959).

2. Cicala, P., and Miele, A., "Brachistocronic Maneuvers of a Constant Mass Aircraft in a Vertical Plane," Journal of Aeronautical Sciences, Vol. 22, No. 4, 1955, pp. 286-288.

3. Landgraff, S. K., "Some Applications of Performance Optimization Techniques to Aircraft," Journal of Aircraft, Vol. 2, No. 2, 1965, pp. 153-154.

4. Bryson, A. E., Jr., Desai, M. N., and Hoffman, W. C., "Energy-State Approximation in Performance Optimization of Supersonic Aircraft," Journal of Aircraft, Vol. 6, No. 6, 1969, pp. 481-488.

5. Miele, A., "An Extension of the Theory of the Optimum Burning Program for the Level Flight of a Rocket Powered Aircraft," Journal of Aeronautical Sciences, Vol. 24, No. 12, 1957, pp. 874-884.

6. Bryson, A. E., Jr., and Lele, M. L., "Minimum Fuel Lateral Turns at Constant Altitude," AIAA Journal, Vol. 7, No. 3, March 1969, pp. 559-560.

7. Hedrick, J. K., and Bryson, A. E., Jr., "Minimum Time Turns for a Supersonic Airplane at Constant Altitude," Journal of Aircraft, Vol. 8, No. 3, 1971, pp. 182-187.

8. Hedrick, J. K., and Bryson, A. E., Jr., "Three-Dimensional Minimum-Time Turns for a Supersonic Aircraft," Journal of Aircraft, Vol. 9, No. 2, 1972, pp. 115-121.

9. Hedrick, J. K., and Bryson, A. E., Jr., "Three-Dimensional Minimum Fuel Turns for a Supersonic Aircraft," Journal of Aircraft, Vol. 9, No. 3, 1972, pp. 223-229.

10. Hoffman, W. C., Zvara, J., and Bryson, A. E., Jr., "Optimum Turns to a Specified Track for a Supersonic Aircraft," Paper No. 32-3, 13th Joint Automatic Control Conference, Stanford, California, August 1972.

11. Bryson, A. E., Jr., and Parsons, M. G., "Constant-Altitude, Minimum-Time Turns to a Line and to a Point for a Supersonic Aircraft with a Constraint on Maximum Velocity," SUDAAR No. 437, Stanford University, Stanford, California, November 1971.

REFERENCES (Cont'd)

12. Parsons, M.G., and Bryson, A.E., Jr., "Three-Dimensional, Minimum-Time Flight Paths to a Point and onto a Line for a Supersonic Aircraft with a Maximum Mach Number Constraint," SUDAAR No. 444, Stanford University, Stanford, California, August 1972.

13. Parsons, M.G., Bryson, A.E., Jr., and Hoffman, W.C., "Long-Range Energy-State Maneuvers for Minimum Time to Specified Terminal Conditions," AIAA Paper No. 73-229, AIAA 11th Aerospace Sciences Meeting, Washington, D.C., January 1973.

14. Spintzyk, J., "Untersuchungen über Zeitoptimale Wende-und Einholmanöver von Überschallflugzeugen," Jahrbuch 1962 der WGLR, pp. 202-217.

15. Vincent, T.L., Lutze, F., and Ishihara, T., "Applications of the Calculus of Variations to Aircraft Performance," NASA CR-498 (1966).

16. Miele, A., "Flight Mechanics," Vol. 1: Theory of Flight Paths. Addison-Wesley Publishing Company, Inc., 1962.

17. Bliss, G.A., "Lectures on Calculus of Variations," University of Chicago Press, 1946.

18. Miele, A., "Theory of Optimum Aerodynamic Shapes," Academic Press, 1965.

19. Leitmann, G., "Optimization Techniques with Applications to Aerospace Systems," Academic Press, 1962.

20. Bryson, A.E., Jr., and Ho, Y.C., "Applied Optimal Control," Ginn and Company, 1969.

21. Speyer, J.L., "Optimization and Control of Nonlinear System with Inflight Constraints," Ph.D. Thesis, Harvard University, Cambridge, Massachusetts, February 1968.

22. MIL-A-8861, "Airplane Strength and Rigidity, Flight Loads," May 1960.

23. Connor, M.A., "Optimization of a Lateral Turn at Constant Height," AIAA Journal, Vol. 5, No. 7, February 1967, pp. 335-338.

24. Bryson, A.E., Jr., and Denham, W.F., "A Steepest-Ascent Method for Solving Optimum Programming Problems," Journal of Applied Mechanics, Vol. 29, June 1962, pp. 247-257.

TABLE 1. OPTIMAL SUBARCS AS FUNCTIONS OF THE LAGRANGE MULTIPLIERS

| $T_w$ | $T_{w_{MAX}}$ | | | $T_{w_{MIN}}$ | | |
|---|---|---|---|---|---|---|
| $\lambda_1$ | $< 0$ | | | $> 0$ | | |
| $C_L$ | $C_{L_{INT}} = \frac{\lambda_2}{2KM\lambda_1}$ | $C_{L_{MAX}}$ | $C_{L_{MIN}}$ | $C_{L_{INT}}$ | $C_{L_{MAX}}$ | $C_{L_{MIN}}$ |
| $\lambda_2$ | $2KC_{L_{MAX}}M\lambda_1 < \lambda_2 < 2KC_{L_{MIN}}M\lambda_1$ | $\leq 2KC_{L_{MAX}}M\lambda_1$ | $\geq 2KC_{L_{MIN}}M\lambda_1$ | | $< 2KC_{L_{AVG}}M\lambda_1$ | $> 2KC_{L_{AVG}}M\lambda_1$ |
| Existence | yes | yes | yes | no | yes | yes |
| Subarc No. | II | I | III | | IV | V |

TABLE 2. AIRCRAFT AND ATMOSPHERIC DATA

Aircraft Data

$W$ = 18,000 lb.

$S$ = 220 sq. ft.

$C_{D0}$ = 0.02 for Simpler Case

= 0.02 $M < 0.93$

= $0.02 + 0.2\,(M - 0.93)$ $0.93 \leq M < 1.03$

= $0.04 + 0.06\,(M - 1.03)$ $1.03 \leq M < 1.10$

= $0.0442 - 0.007\,(M - 1.10)$ $1.10 \leq M$

Shown in Fig. 5

$K$ = 0.2 for Simpler Case

= 0.2 $M < 1.15$

= $0.2 + 0.246\,(M - 1.15)$ $1.15 \leq M$

Shown in Fig. 6

$Tw_{MAX}$ = constant with altitude and speed for Simpler Case

$= 0.0405\,(1 + 0.597297M^2)\,Sw\,e^{-1.4\eta}$

$Tw_{MAX}$ = 0.5 at altitude of 20,000 ft. and speed of Mach 0.9

$Tw_{MIN} = 0$

Atmospheric Data

Reference and starting altitude: 20,000 ft.

$p$ = 972.49 psf

$a$ = 1037.26 fps

$\varkappa = 1.4$

Others

$g = 32.1741$ ft/sec$^2$

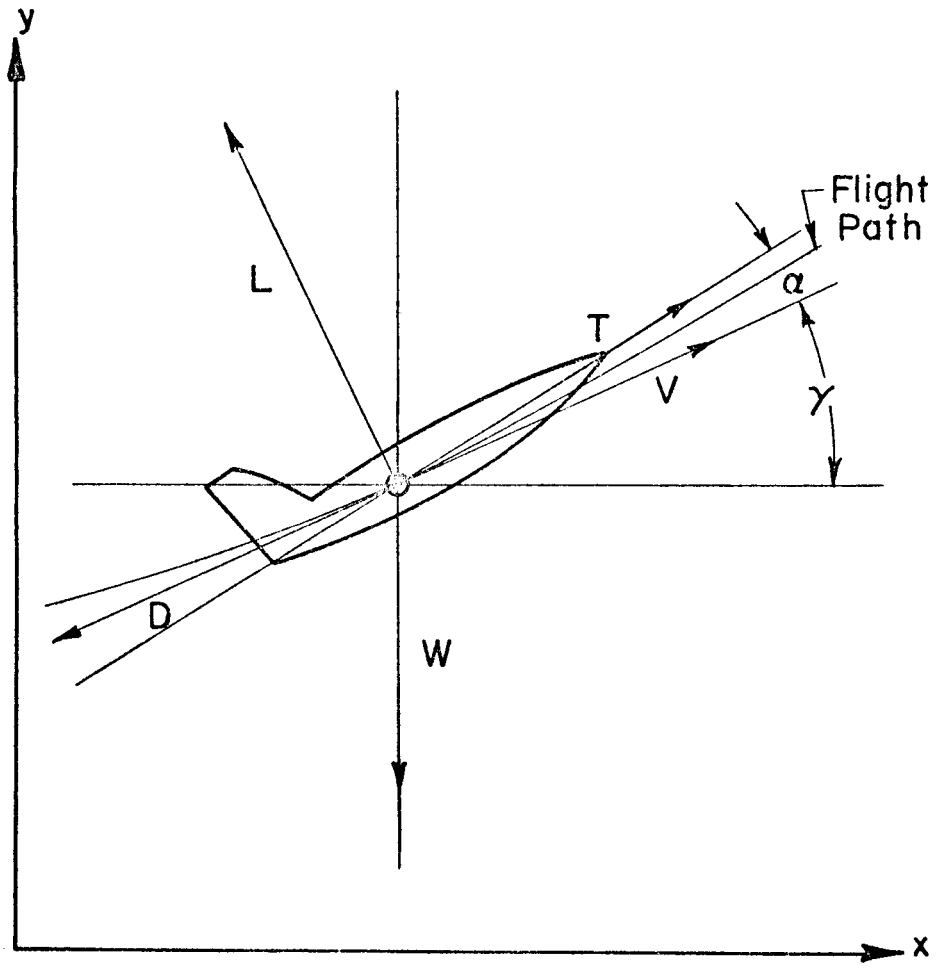


FIG. I COORDINATE AXES AND FORCES

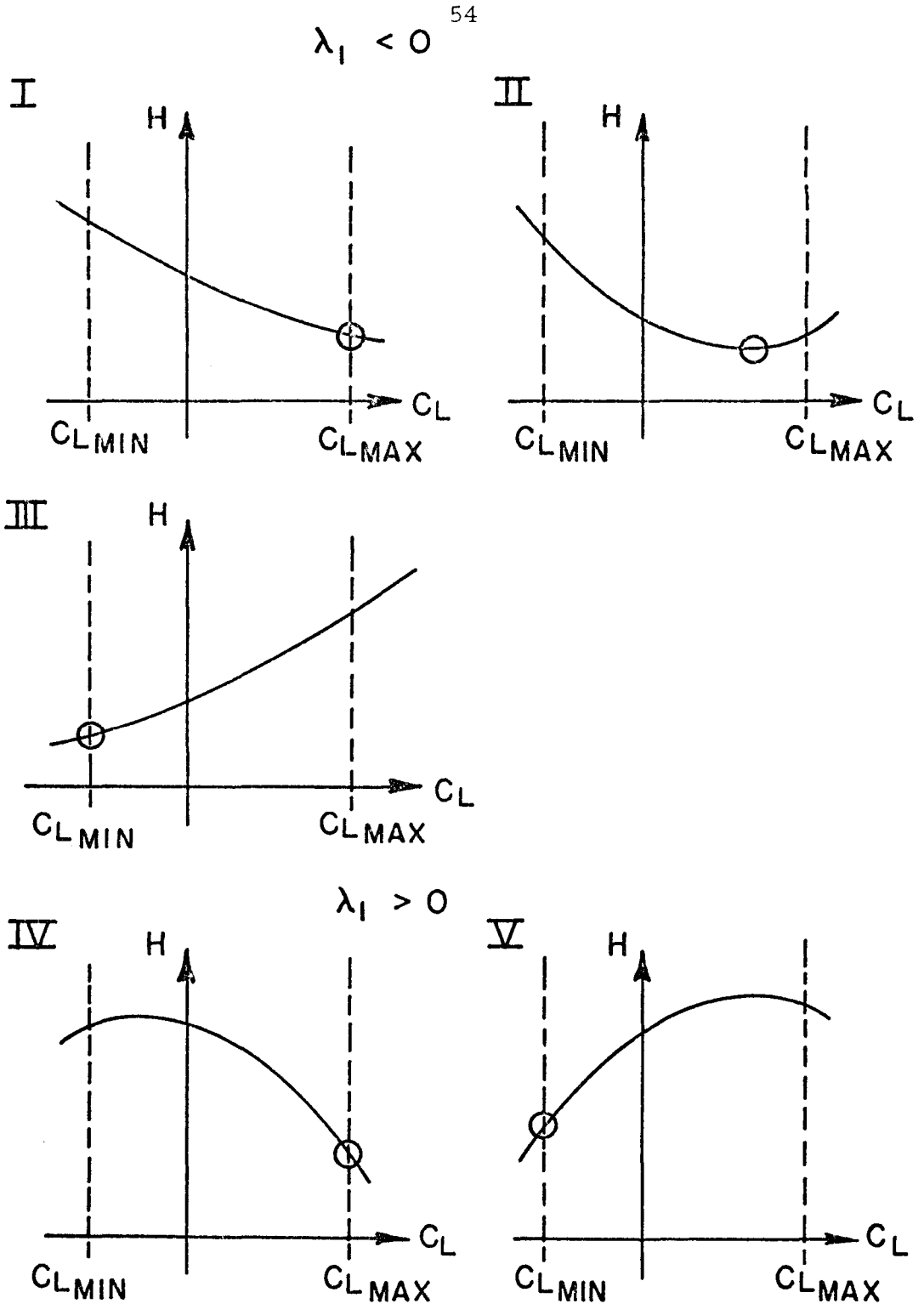
λ1 < 0
I
H
CL
CLMIN
CLMAX
II
H
CL
CLMIN
CLMAX
III
H
CL
CLMIN
CLMAX
λ1 > 0
IV
H
CL
CLMIN
CLMAX
V
H
CL
CLMIN
CLMAX

FIG. 2 H VS. $C_L$

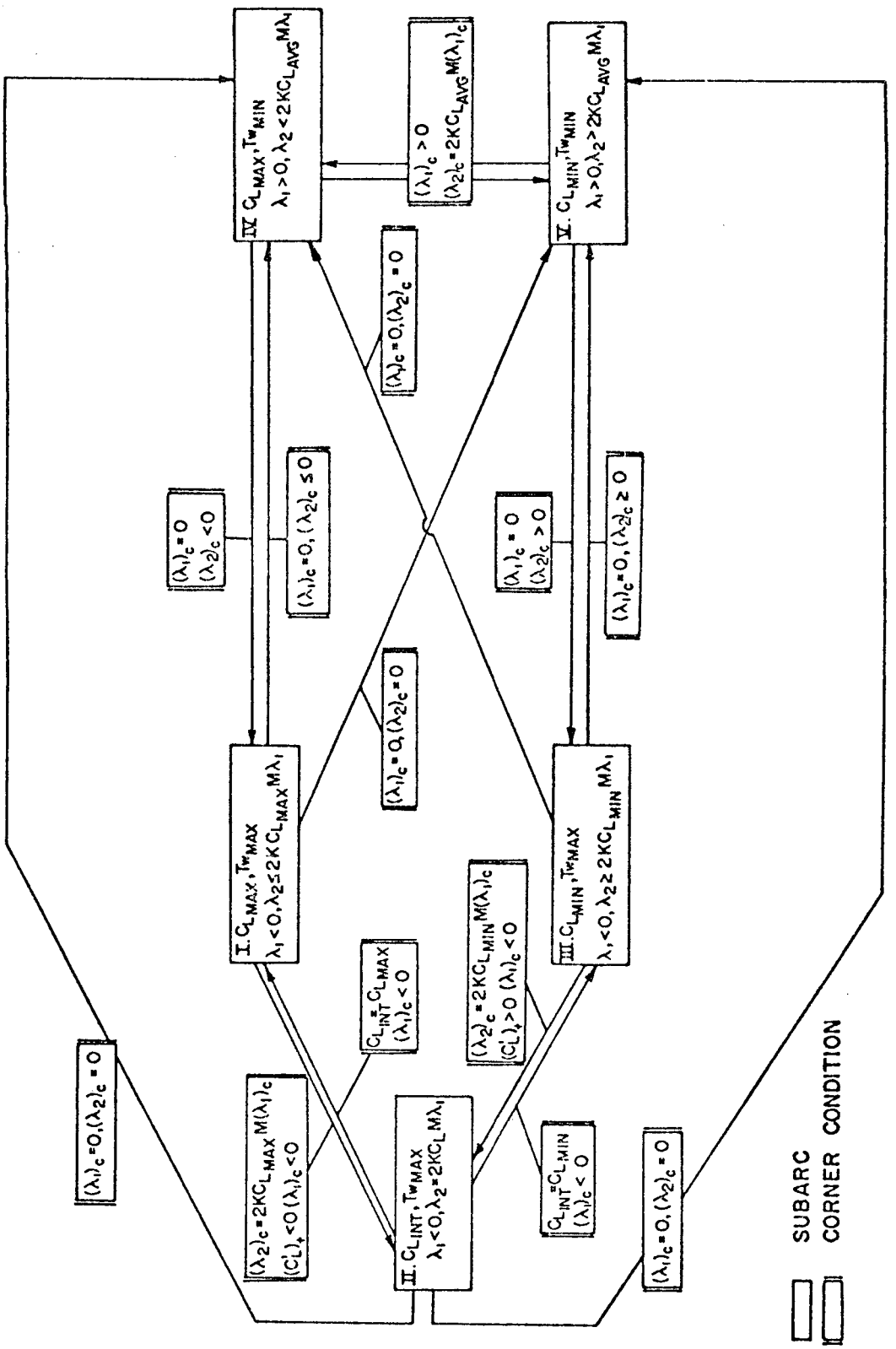


FIG. 3 SEQUENCES OF SUBARCS

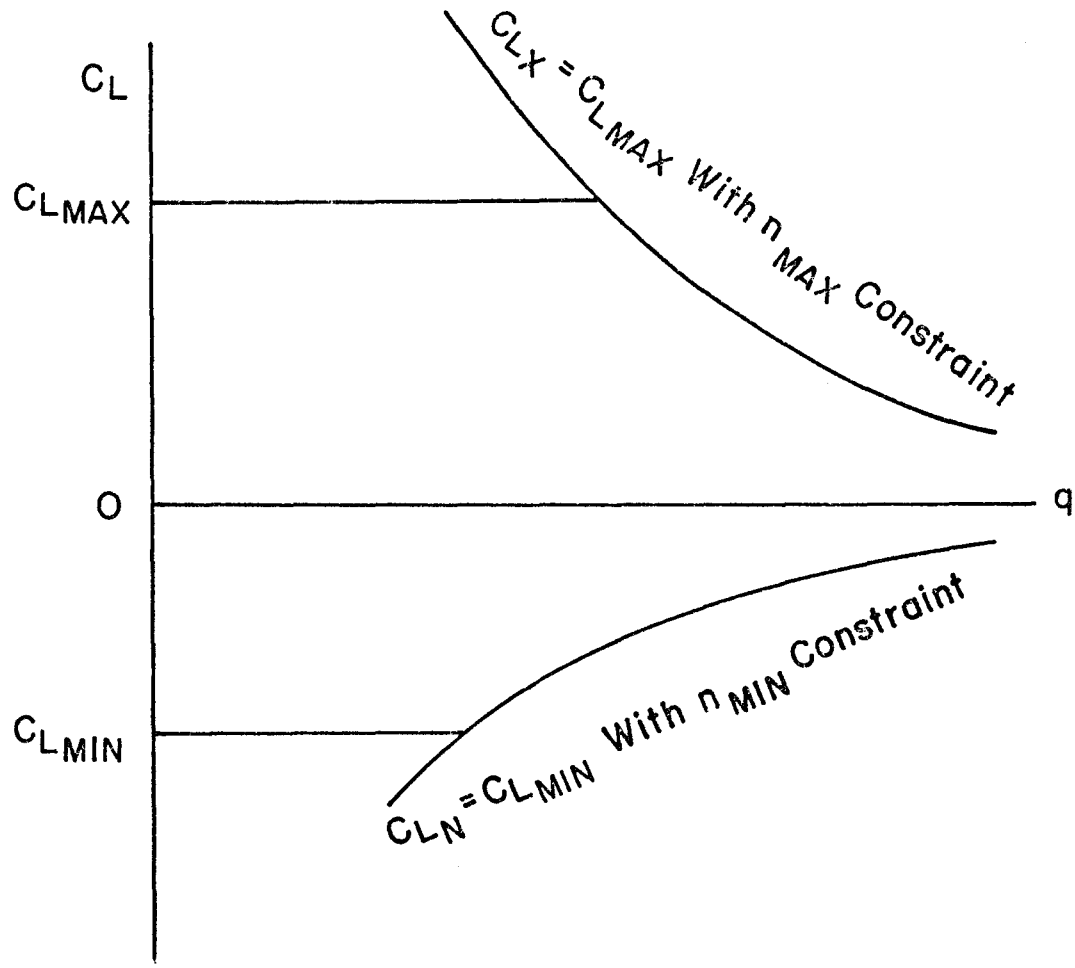


FIG. 4 LIFT COEFFICIENT CONSTRAINTS AS FUNCTIONS OF DYNAMIC PRESSURE

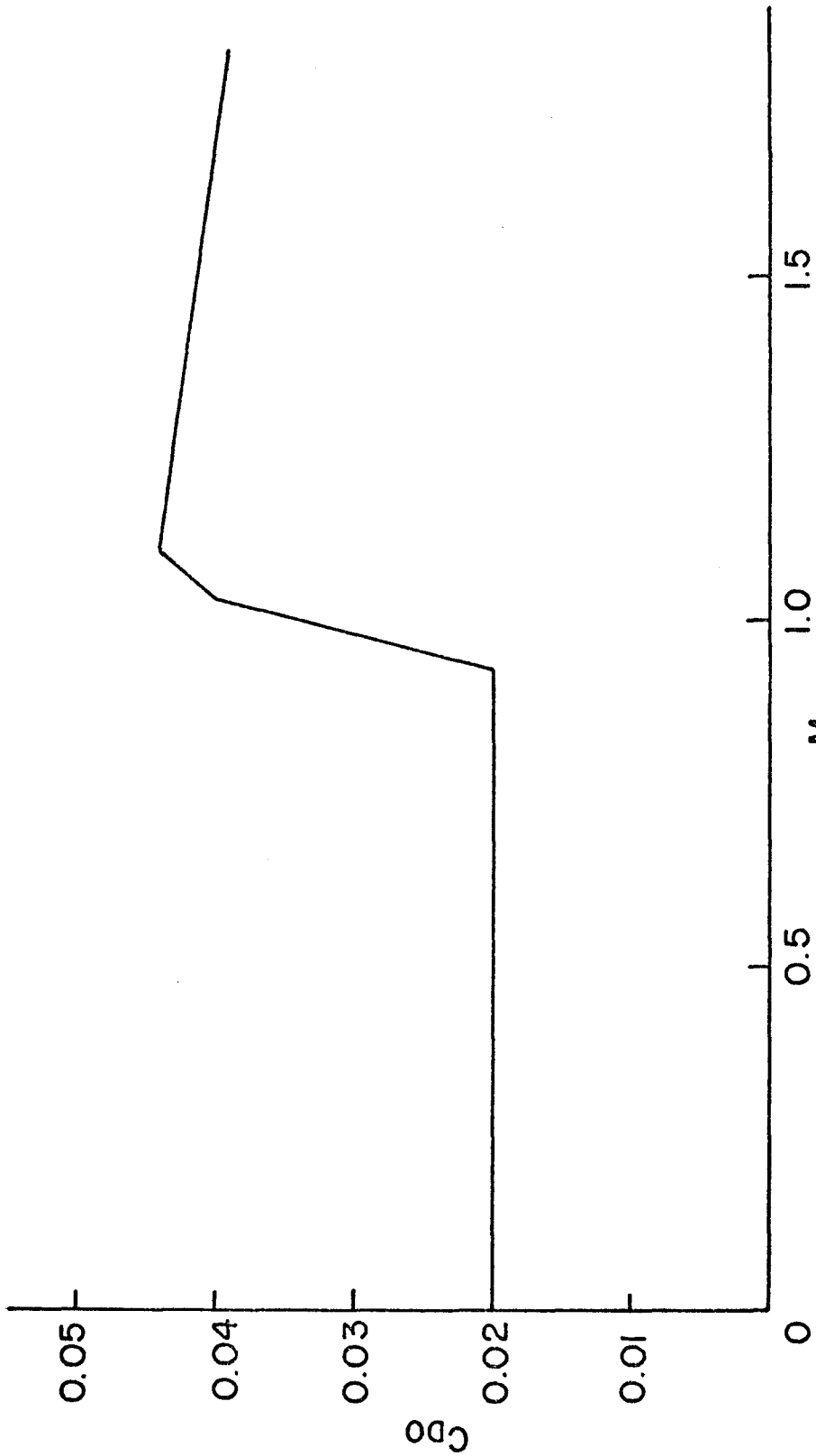


FIG. 5 $C_{DO}$ VS. M

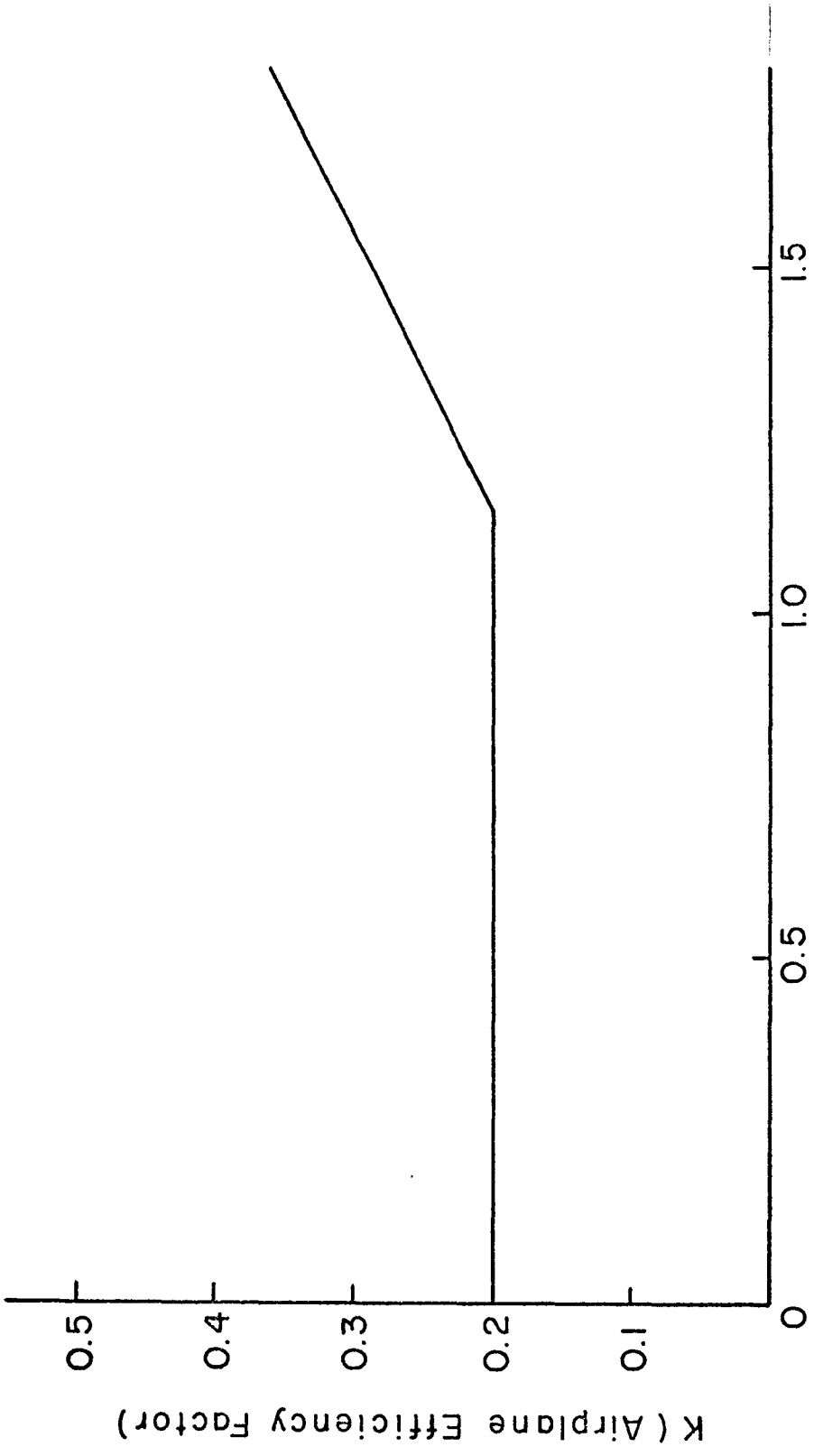


FIG. 6 K VS. M

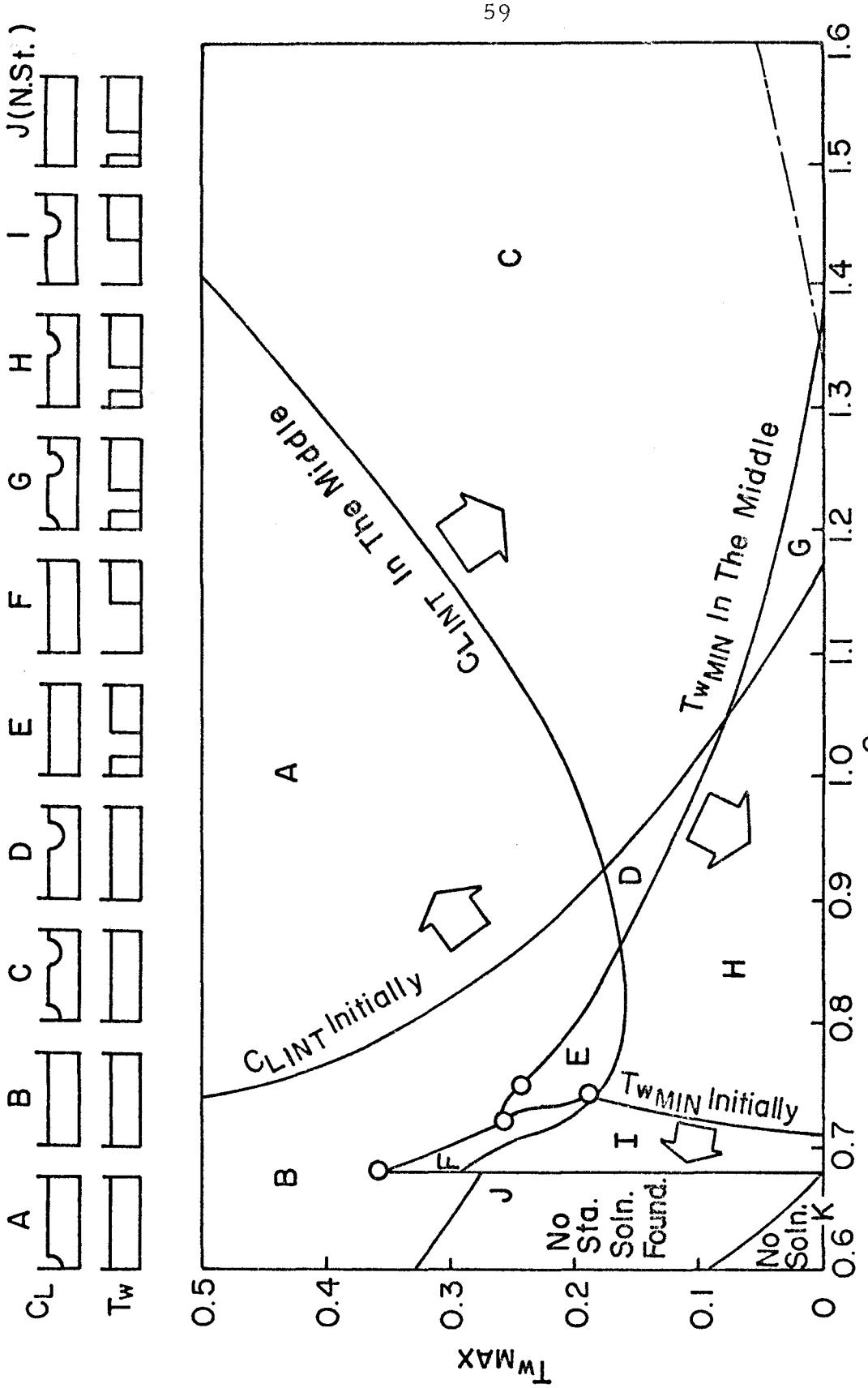


FIG. 7 CONTROL HISTORY MAP ($\lambda_3 = 0$, $\lambda_4 = 0$)

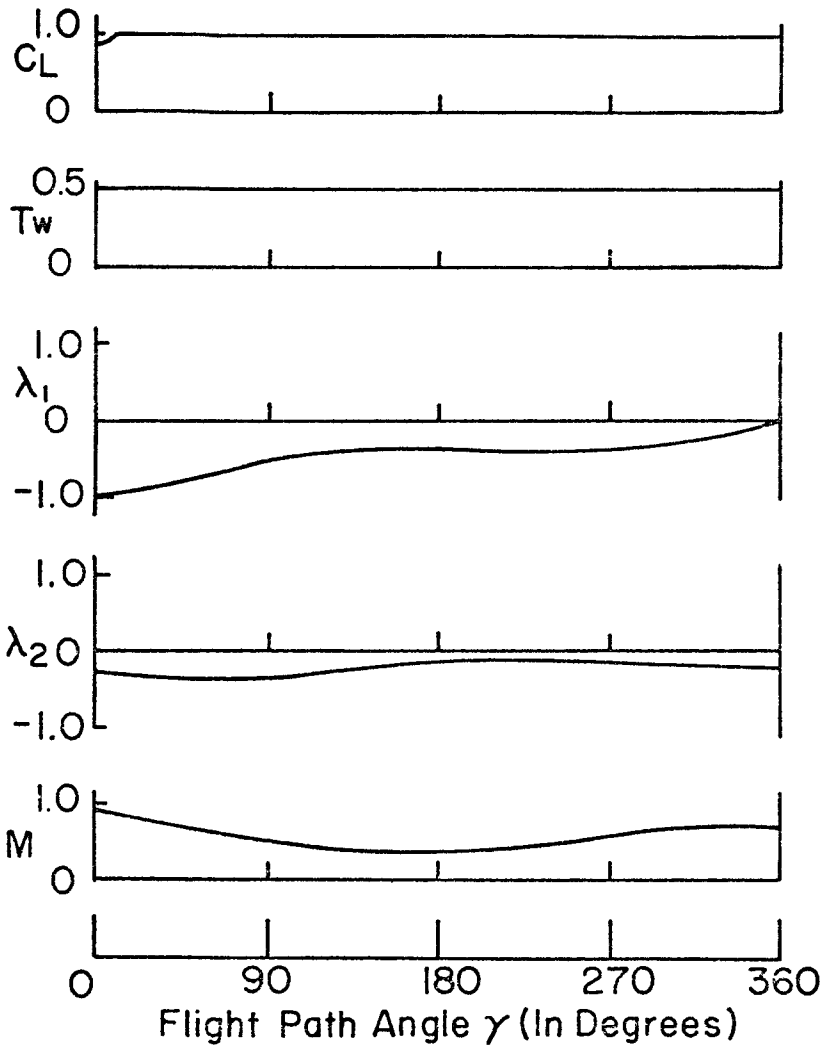


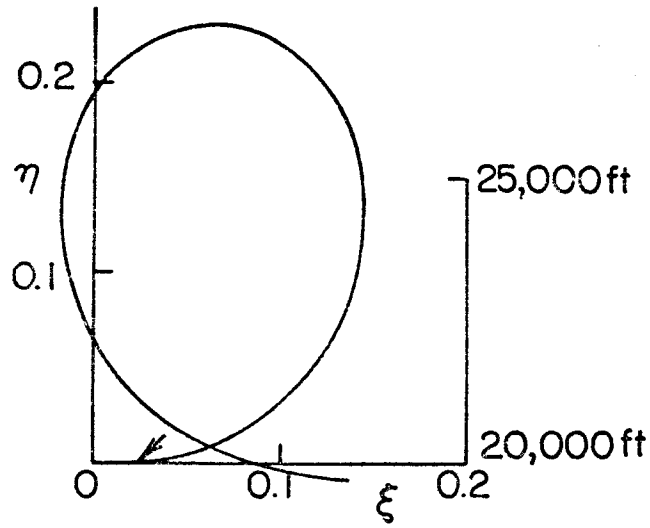


| | | | |
|---|---|---|---|
| Initial $C_L$ | | 0.8856 | |
| Final Values | | | |
| Time | $t_f$ | 39.42 | sec |
| Speed | $M_f$ | 0.6921 | M |
| Range | $x_f$ | 4428 | ft |
| Height | $y_f$ | -205.4 | ft |
| Maximum Normal Acceleration | | 6.34 | g |

FIG. 8-a HISTORY OF CONTROL AND STATE VARIABLES, LAGRANGE MULTIPLIERS: $C_{L_{MAX}}$=1.0, $Tw_{MAX}$ = 0.5 (CASE A)

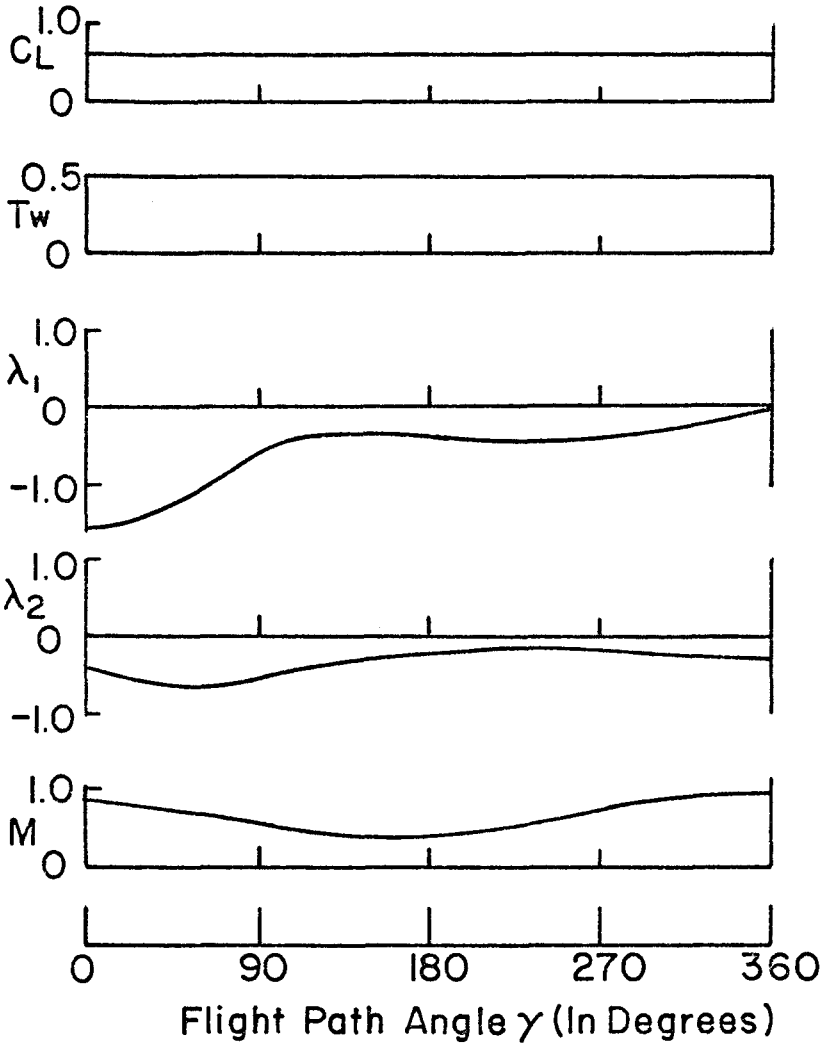


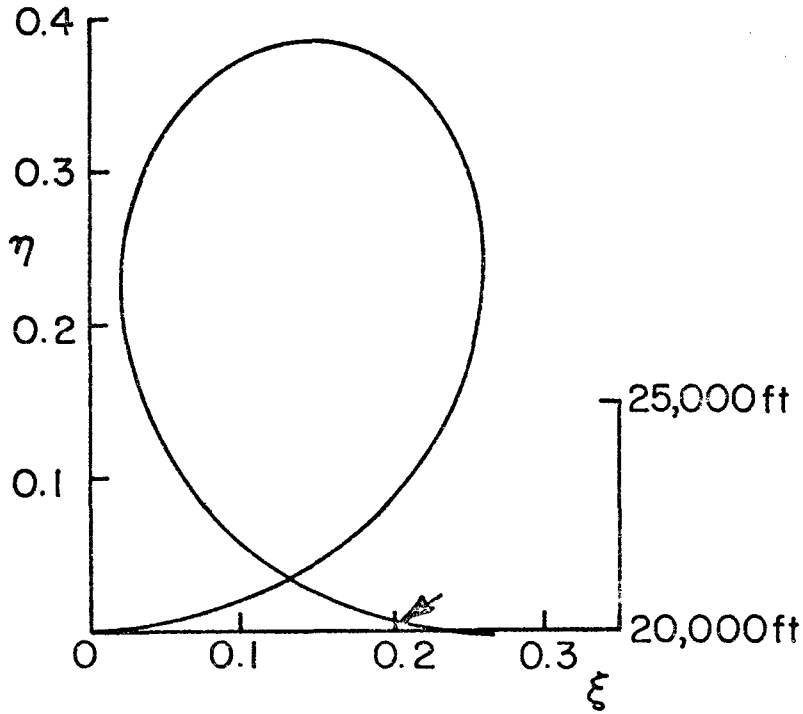


Final Values

| | | | |
|---|---|---|---|
| Time | $t_f$ | 55.46 | sec |
| Speed | $M_f$ | 0.9707 | M |
| Range | $x_f$ | 8768 | ft |
| Height | $y_f$ | -28.12 | ft |
| Maximum Normal Acceleration | | 4.78 | g |

FIG.8-b HISTORY OF CONTROL AND STATE VARIABLES, LAGRANGE MULTIPLIERS: $C_{L_{MAX}} = 0.6$, $T_{w_{MAX}} = 0.5$ (CASE B)

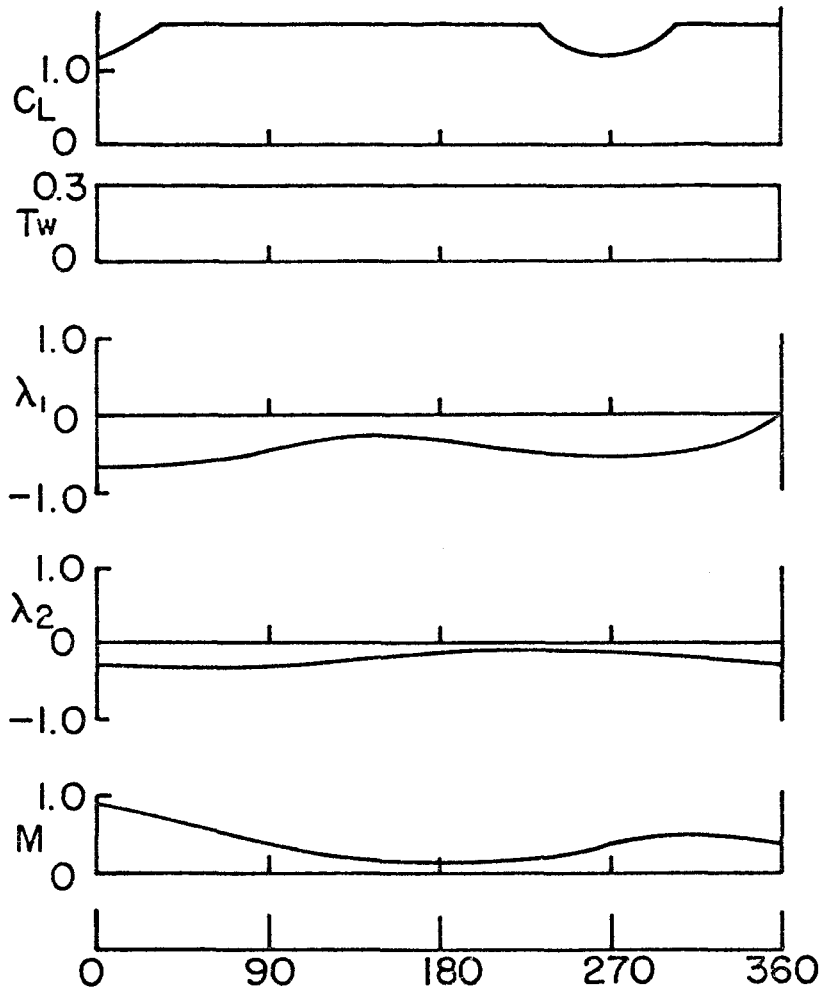


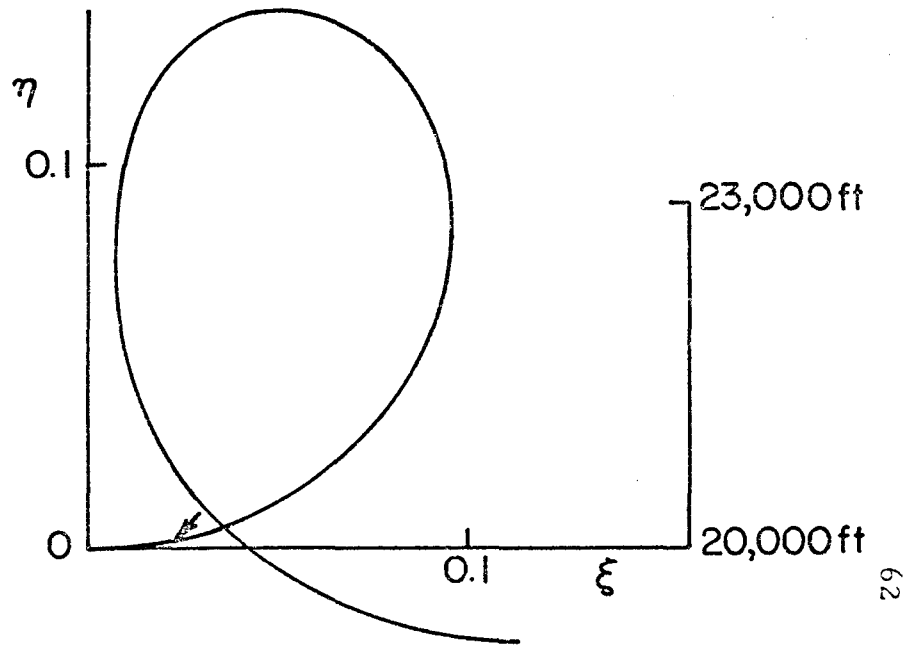


| | | | |
|---|---|---|---|
| Initial $C_L$ | | 1.121 | |
| Final Values | | | |
| Time | $t_f$ | 34.65 | sec |
| Speed | $M_f$ | 0.4327 | M |
| Range | $x_f$ | 3777 | ft |
| Height | $y_f$ | -797.4 | ft |
| Maximum Normal Acceleration | | 7.66 | g |

FIG. 8-c HISTORY OF CONTROL AND STATE VARIABLES, LAGRANGE MULTIPLIERS: $C_{L_{MAX}} = 1.6$, $T_{W_{MAX}} = 0.3$ (CASE C)

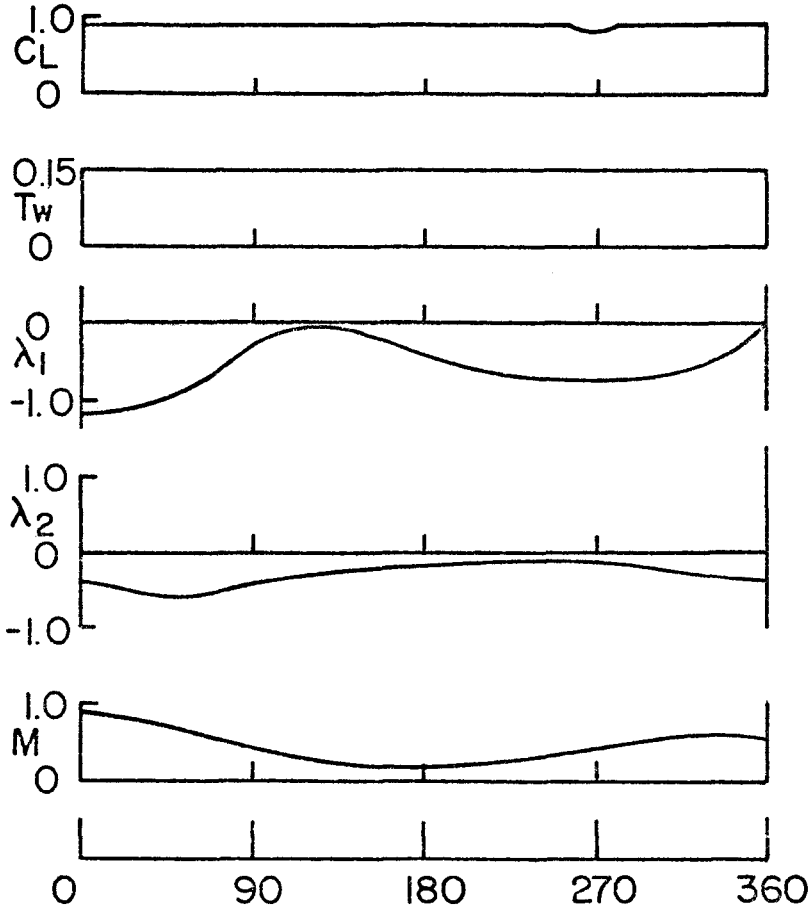


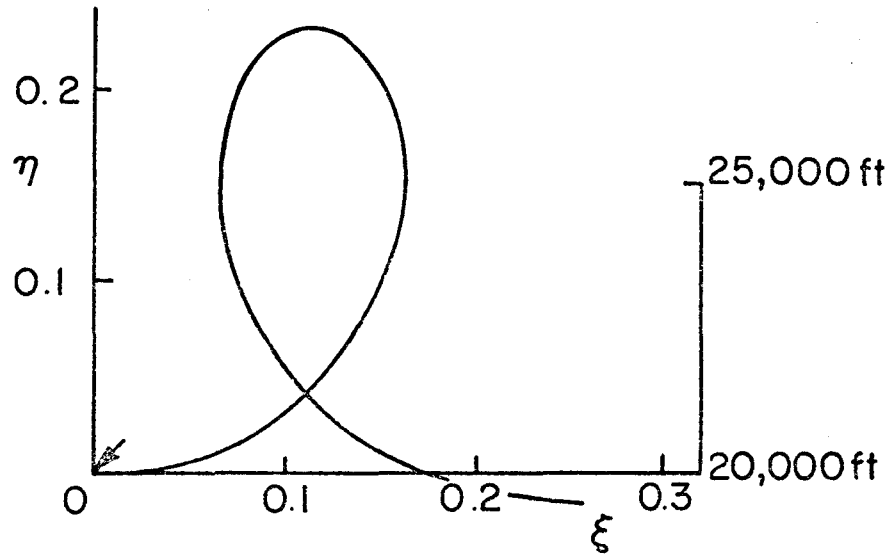


| Final Value | | | |
|---|---|---|---|
| Time | $t_f$ | 50.59 | sec |
| Speed | M | 0.5834 | M |
| Range | $x_f$ | 8603 | ft |
| Altitude | $y_f$ | -593.2 | ft |
| Maximum Normal Acceleration | ↙ | 6.07 | g |

FIG.8-dHISTORY OF CONTROL AND STATE VARIABLES, LAGRANGE MULTIPLIERS: $C_{L_{MAX}} = 0.9$ , $T_{w_{MAX}} = 0.15$ (CASE D)

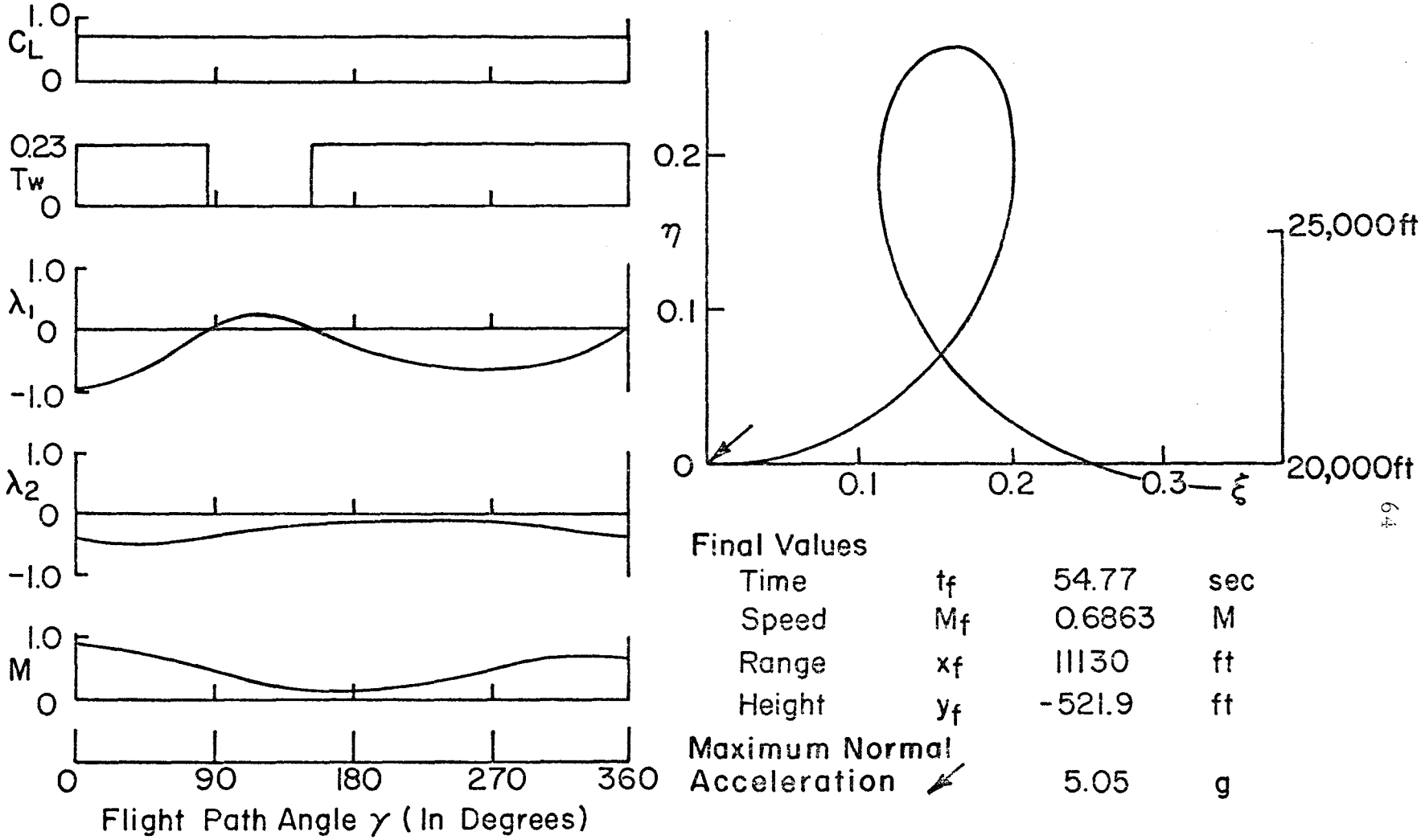


| Final Values | | | |
|---|---|---|---|
| Time | $t_f$ | 54.77 | sec |
| Speed | $M_f$ | 0.6863 | M |
| Range | $x_f$ | 11130 | ft |
| Height | $y_f$ | -521.9 | ft |
| Maximum Normal Acceleration | | 5.05 | g |

FIG. 8-e HISTORY OF CONTROL AND STATE VARIABLES, LAGRANGE MULTIPLIERS: $C_{L_{MAX}} = 0.75$, $Tw_{MAX} = 0.23$ (CASE E)

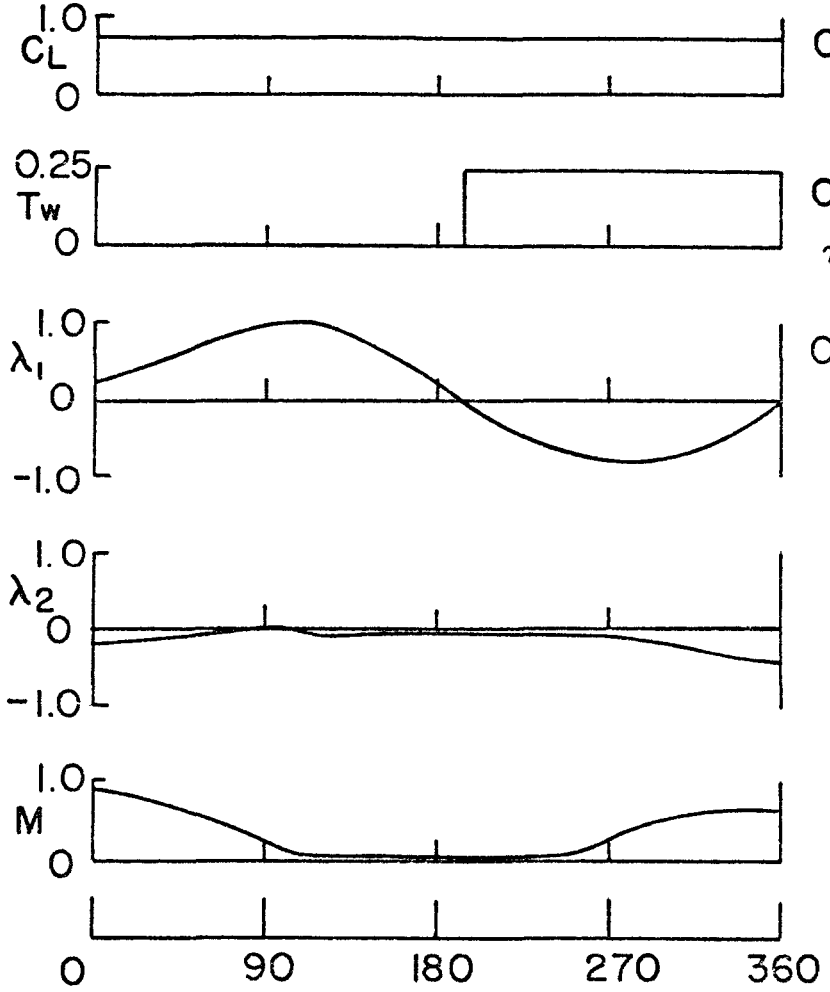


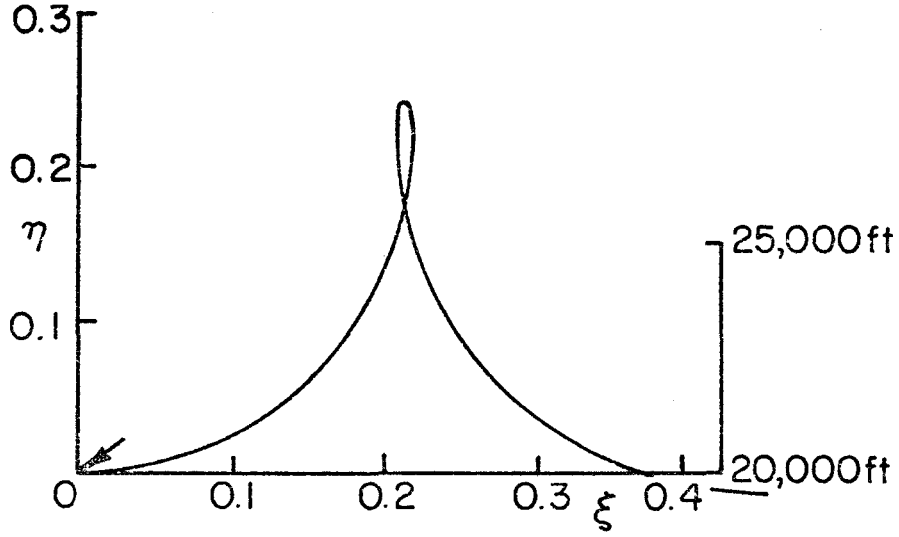


Final Values

| | | | |
|---|---|---|---|
| Time | $t_f$ | 55.63 | sec |
| Speed | $M_f$ | 0.6708 | M |
| Range | $x_f$ | 15210 | ft |
| Height | $y_f$ | -488.2 | ft |
| Maximum Normal Acceleration | | 4.85 | g |

FIG. 8-f HISTORY OF CONTROL AND STATE VARIABLES, LAGRANGE MULTIPLIERS: $C_{L_{MAX}} = 0.72$, $T_{w_{MAX}} = 0.25$ (CASE F)

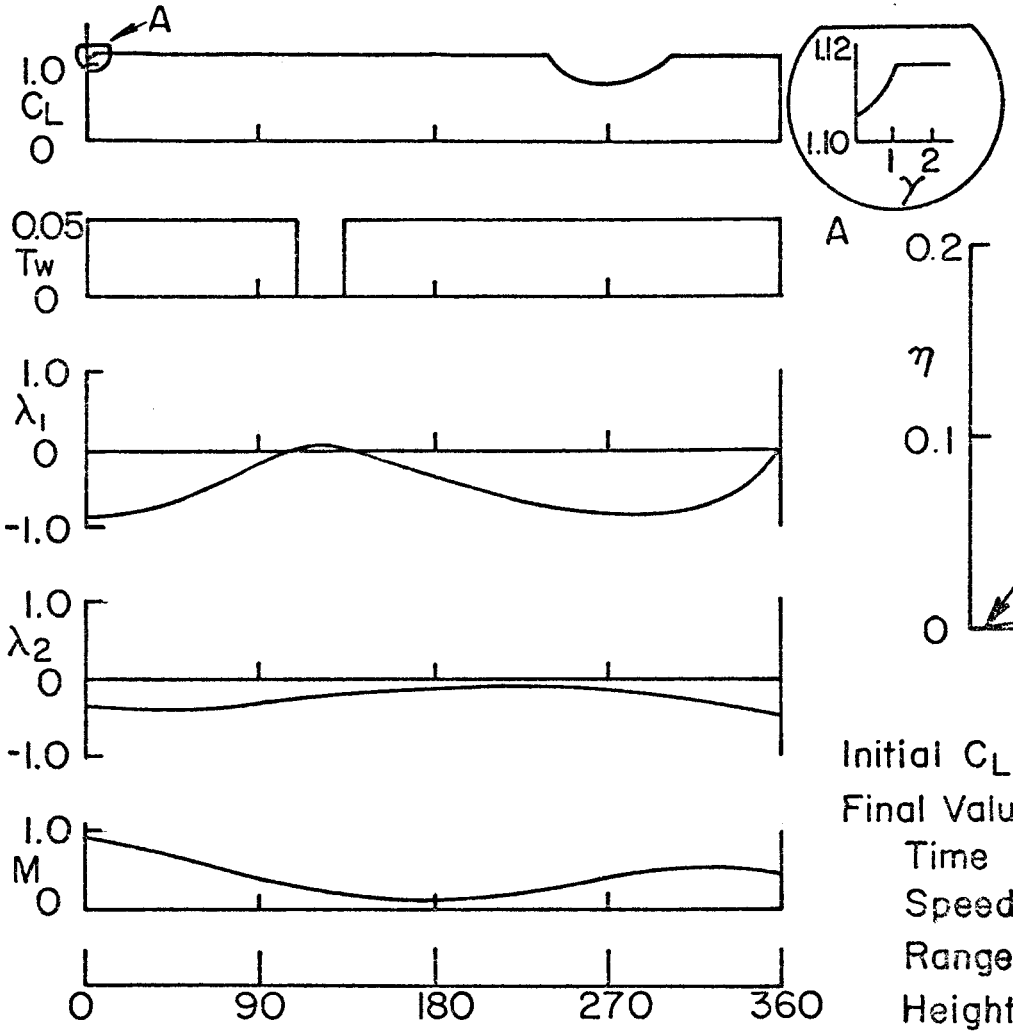


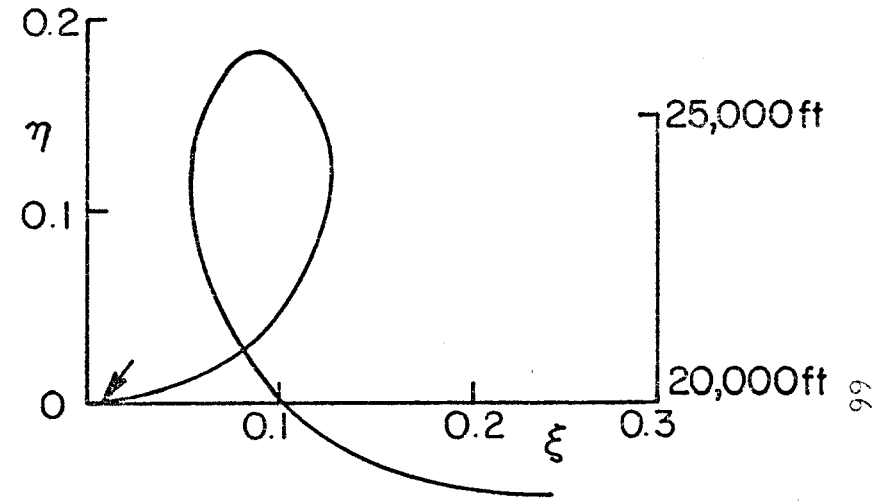


| | | | |
|---|---|---|---|
| Initial $C_L$ | | 1.107 | |
| Final Values | | | |
| Time | $t_f$ | 47.05 | sec |
| Speed | $M_f$ | 0.4817 | M |
| Range | $x_f$ | 7363 | ft |
| Height | $y_f$ | -1508 | ft |
| Maximum Normal Acceleration | | 7.47 | g |

FIG.8-g HISTORY OF CONTROL AND STATE VARIABLES, LAGRANGE MULTIPLIERS: $C_{L_{MAX}} = 1.12$, $T_{W_{MAX}} = 0.05$ (CASE G)

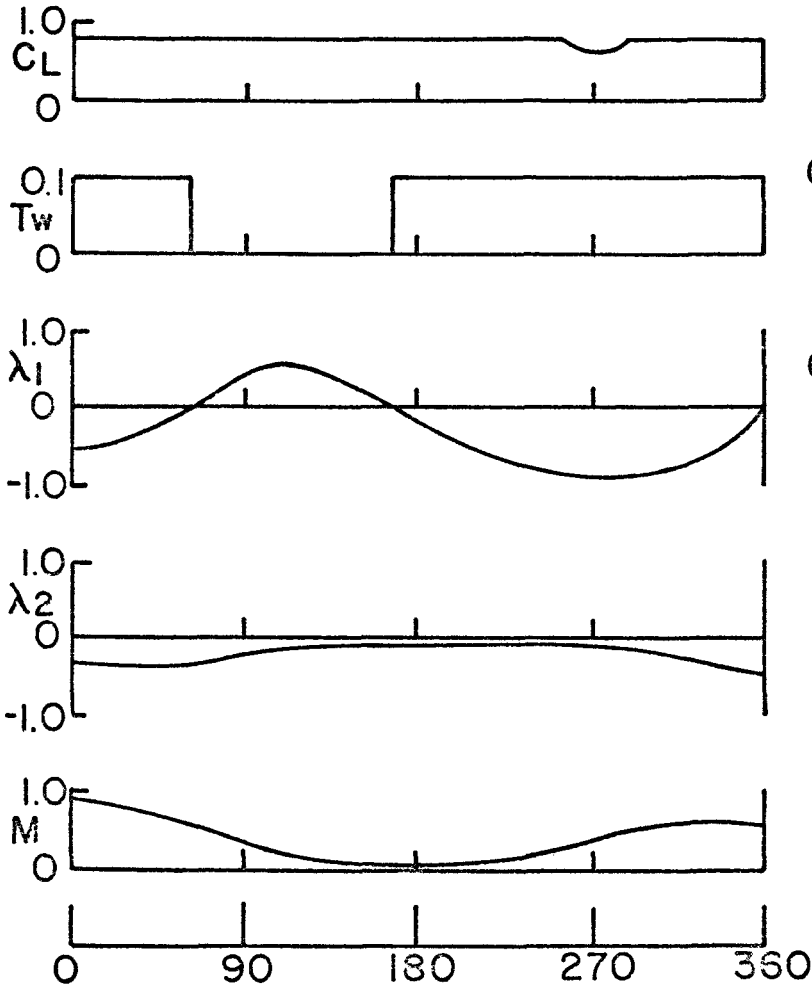


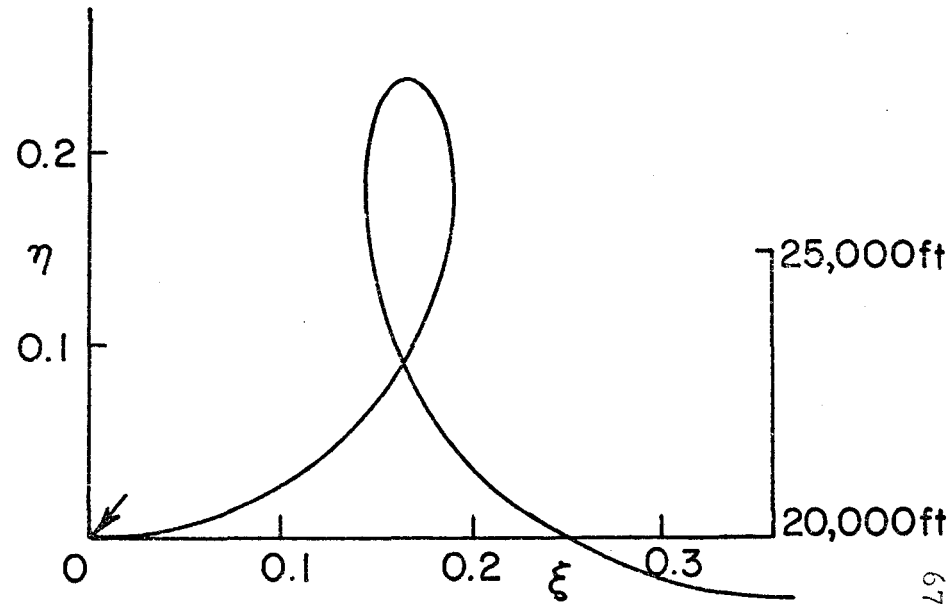


67

| Final Values | | | |
|---|---|---|---|
| Time | $t_f$ | 55.56 | sec |
| Speed | $M_f$ | 0.5962 | M |
| Range | $x_f$ | 12260 | ft |
| Height | $y_f$ | -1015 | ft |
| Maximum Normal Acceleration | ↙ | 5.39 | g |

FIG.8-h HISTORY OF CONTROL AND STATE VARIABLES, LAGRANGE MULTIPLIERS: $C_{L_{MAX}} = 0.8$, $T_{w_{MAX}} = 0.1$ (CASE H)

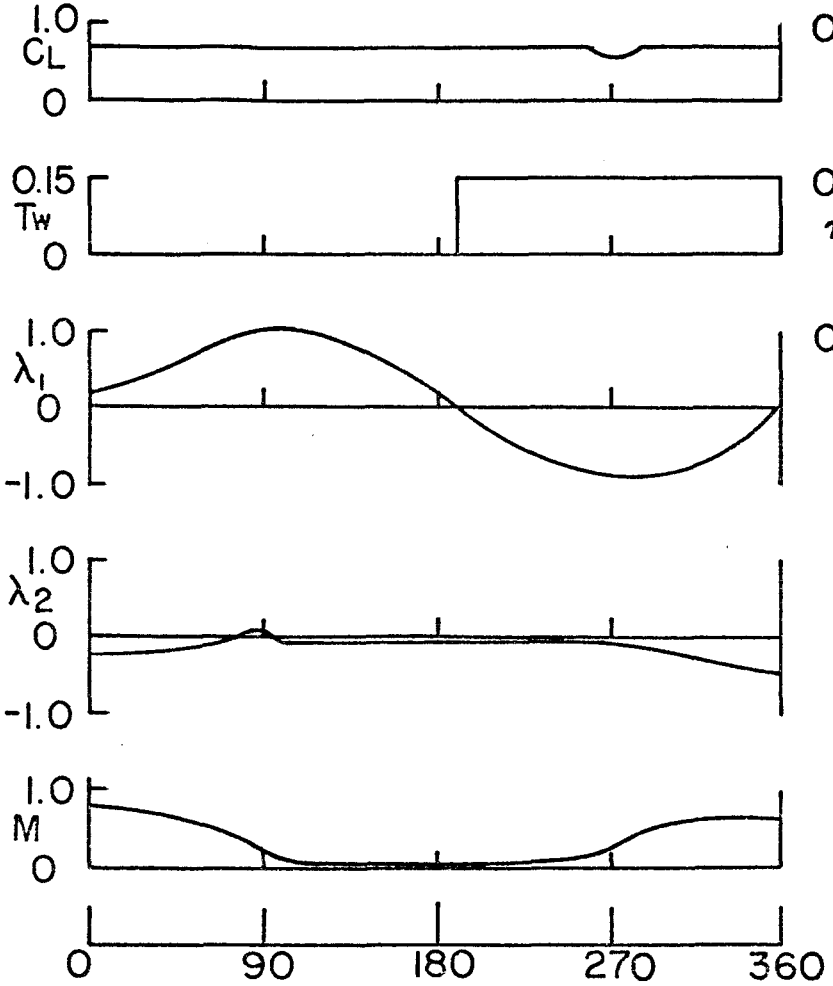


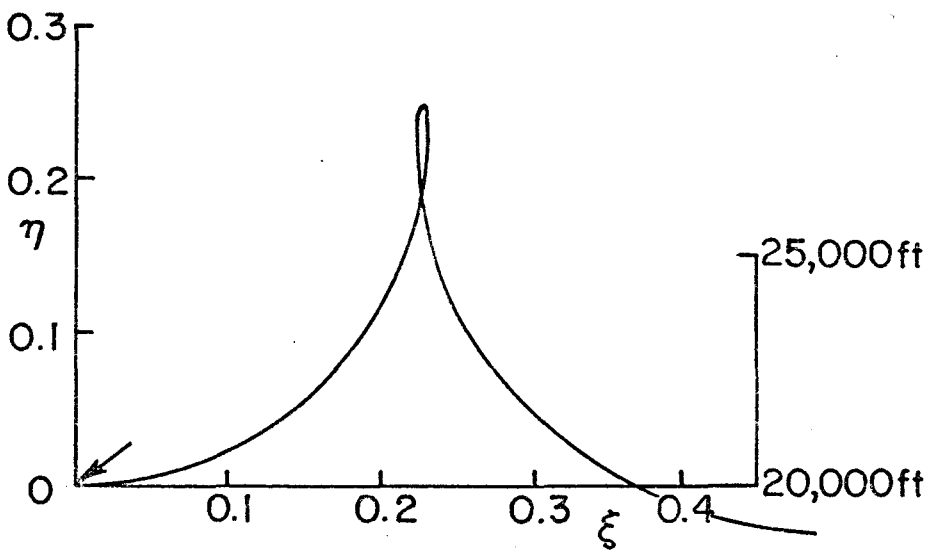


| Final Value | | | |
|---|---|---|---|
| Time | $t_f$ | 58.29 | sec |
| Speed | $M_f$ | 0.6483 | M |
| Range | $x_f$ | 16280 | ft |
| Height | $y_f$ | -959.0 | ft |
| Maximum Normal Acceleration | ↙ | 4.72 | g |

FIG. 8-i HISTORY OF CONTROL AND STATE VARIABLES, LAGRANGE MULTIPLIERS: $C_{L_{MAX}} = 0.7$, $T_{W_{MAX}} = 0.15$ ( CASE I )

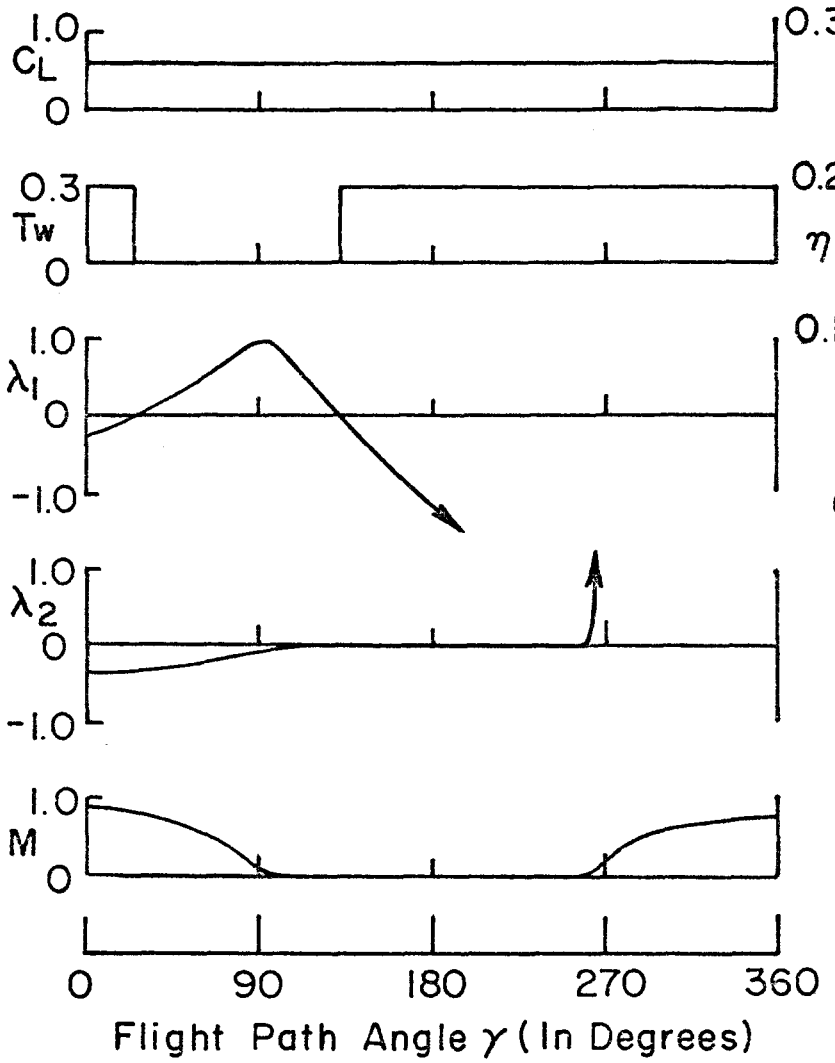


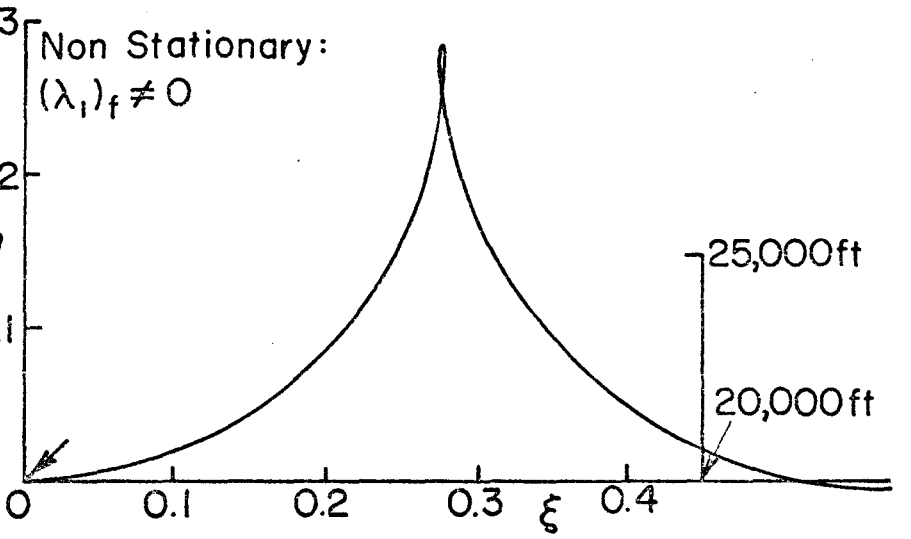


Final Values

| | | | |
|---|---|---|---|
| Time | $t_f$ | 59.71 | sec |
| Speed | $M_f$ | 0.7559 | M |
| Range | $x_f$ | 19130 | ft |
| Altitude | $y_f$ | -80.49 | ft |
| Maximum Normal Acceleration | ↙ | 4.04 | g |



FIG. 8-j HISTORY OF CONTROL AND STATE VARIABLES, LAGRANGE MULTIPLIERS: $C_{L_{MAX}} = 0.6$, $T_{W_{MAX}} = 0.3$ (CASE J)

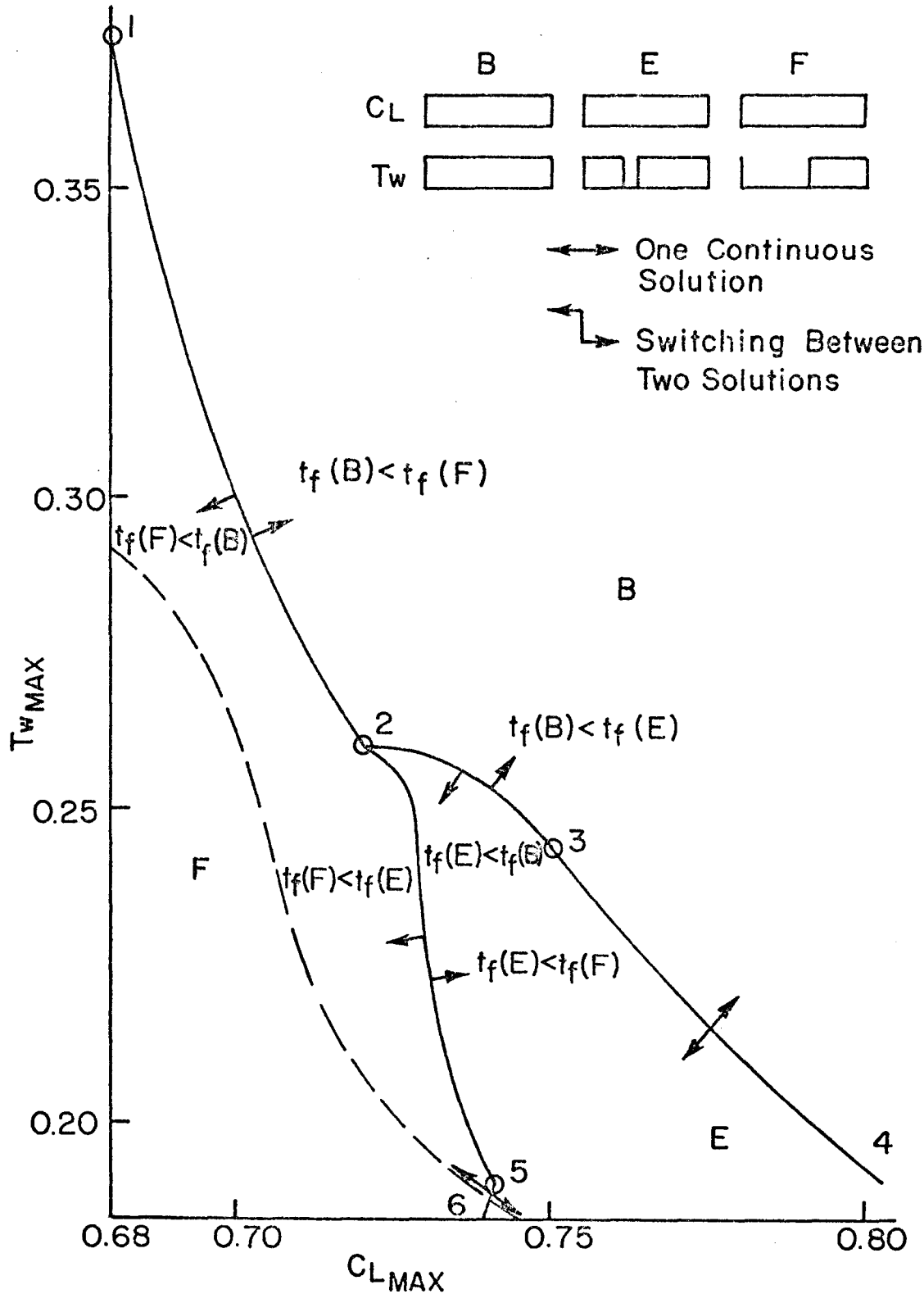


FIG. 9 MULTIPLE SOLUTION REGION

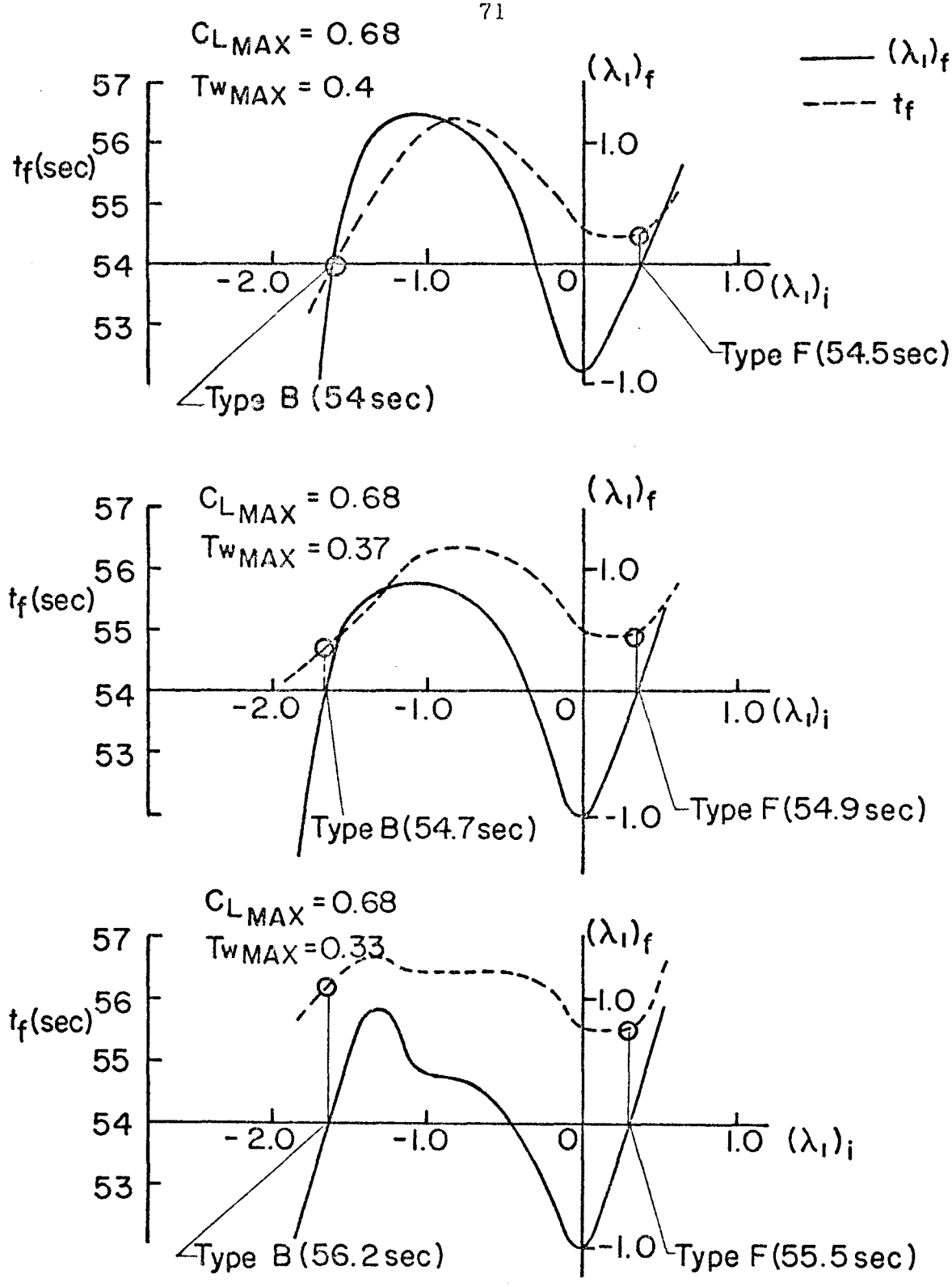


FIG. 10 SWITCHING FROM ONE SOLUTION TO THE OTHER

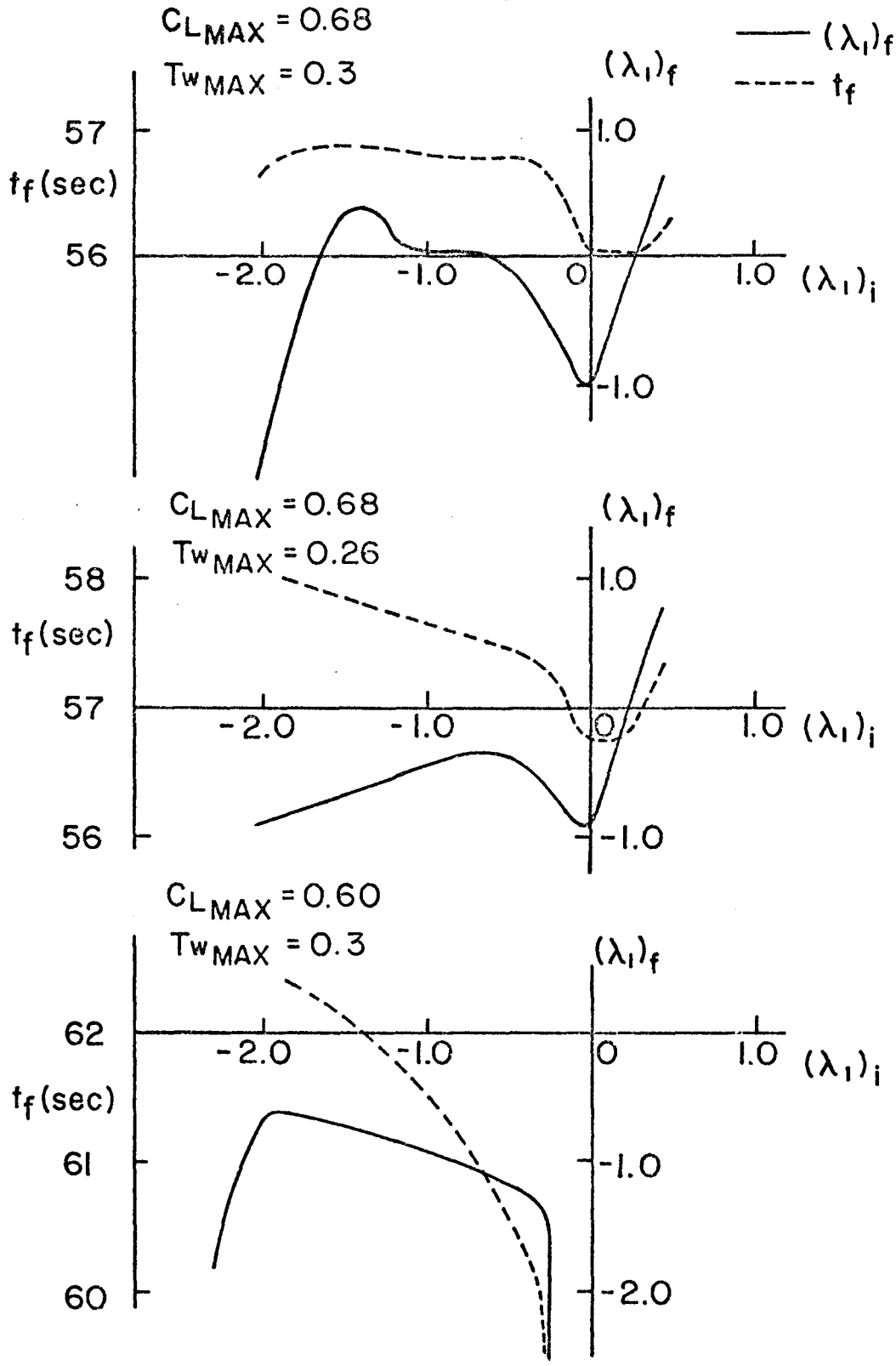


FIG. 11 $(\lambda_1)_f$ VS. $(\lambda_1)_i$ IN SMALL $C_{L_{MAX}}$ AND MEDIUM $Tw_{MAX}$ REGION

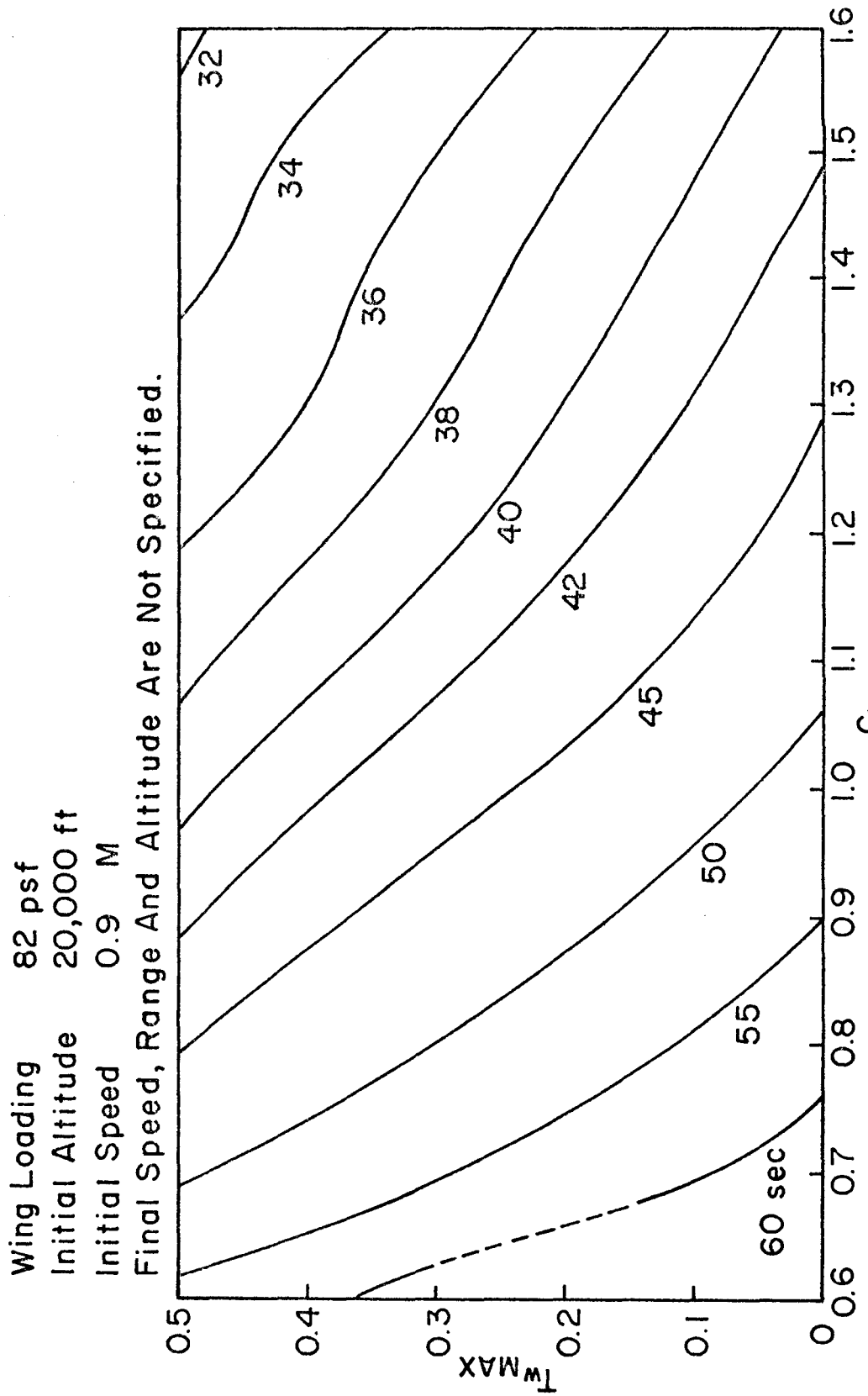


FIG. 12 CONTOUR OF TIME FOR MANEUVER

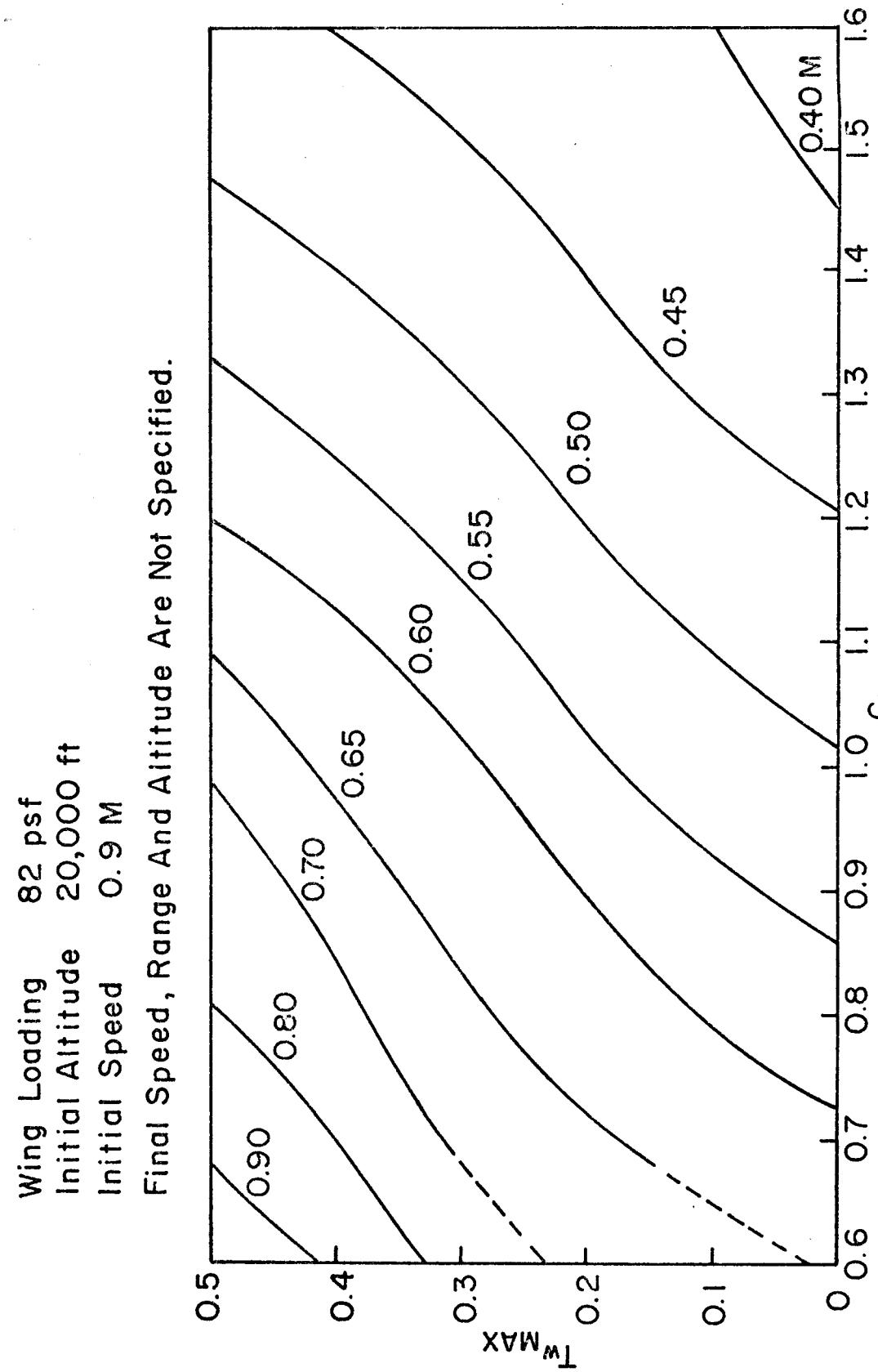


FIG. 13 CONTOUR OF FINAL MACH NUMBER

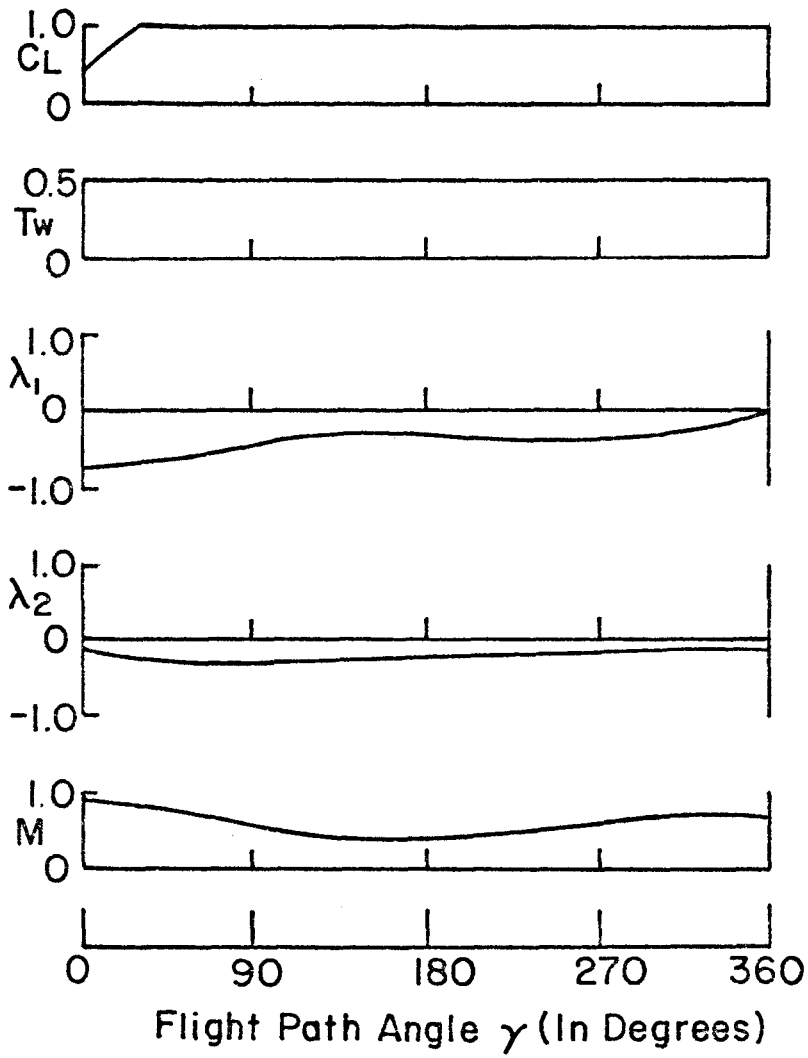


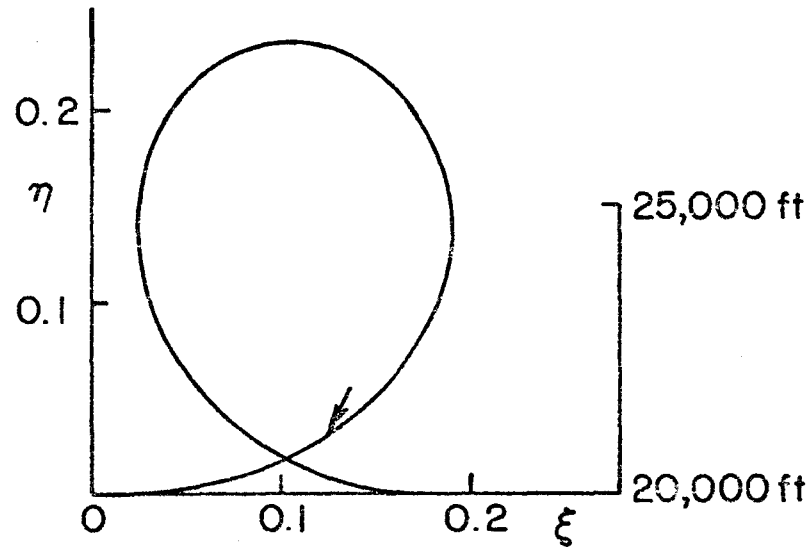


| | | | |
|---|---|---|---|
| Initial $C_L$ | | 0.4 | |
| Final Values | | | |
| Time | $t_f$ | 40.14 | sec |
| Speed | $M_f$ | 0.6963 | M |
| Range | $x_f$ | 5776 | ft |
| Altitude | $y_f$ | 30.32 | ft |
| Maximum Normal Acceleration | | 5.80 | g |

FIG. 14 HISTORY OF CONTROL AND STATE VARIABLES, LAGRANGE MULTIPLIERS: $C_{L_{MAX}} = 1.0$, $Tw_{MAX} = 0.5$, $\lambda_3 = -0.7390$, $\lambda_4 = 0$

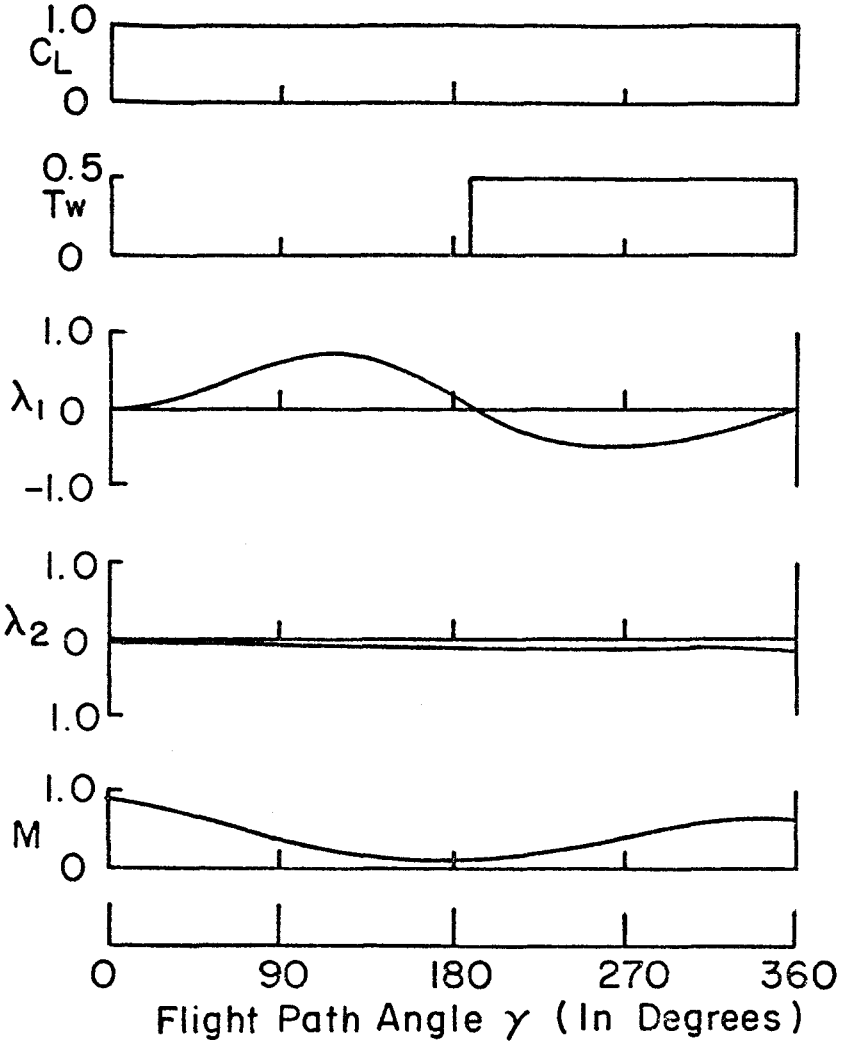


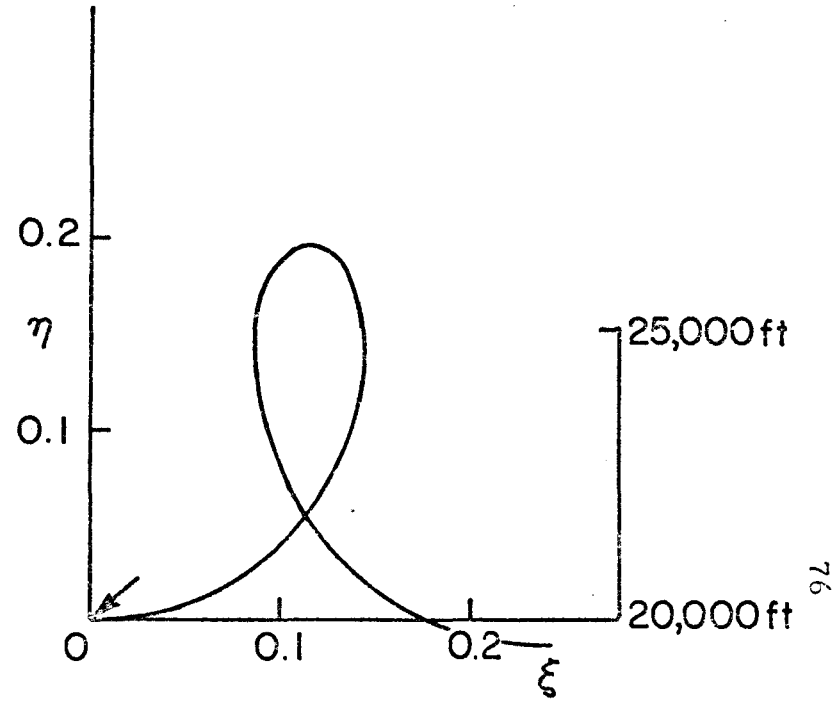


| | | | |
|---|---|---|---|
| Initial $\lambda_1$ | | 0.0 | |
| Final Values | | | |
| Time | $t_f$ | 44.19 | sec |
| Speed | $M_f$ | 0.6396 | M |
| Range | $x_f$ | 8152 | ft |
| Altitude | $y_f$ | -442.4 | ft |
| Maximum Normal Acceleration | ↙ | 6.74 | g |

FIG. 15 HISTORY OF CONTROL AND STATE VARIABLES, LAGRANGE MULTIPLIERS: $C_{L_{MAX}} = 1.0$, $T_{w\,MAX} = 0.5$, $\lambda_3 = -0.710$, $\lambda_4 = 0$

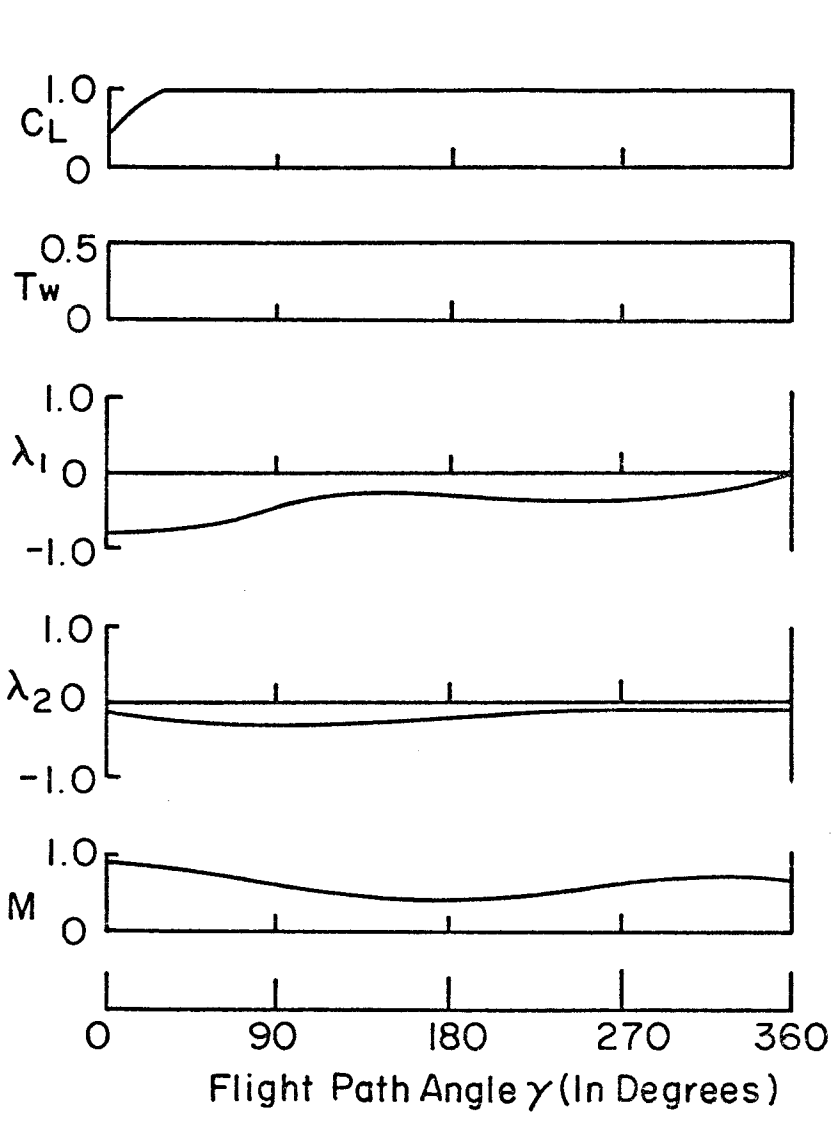


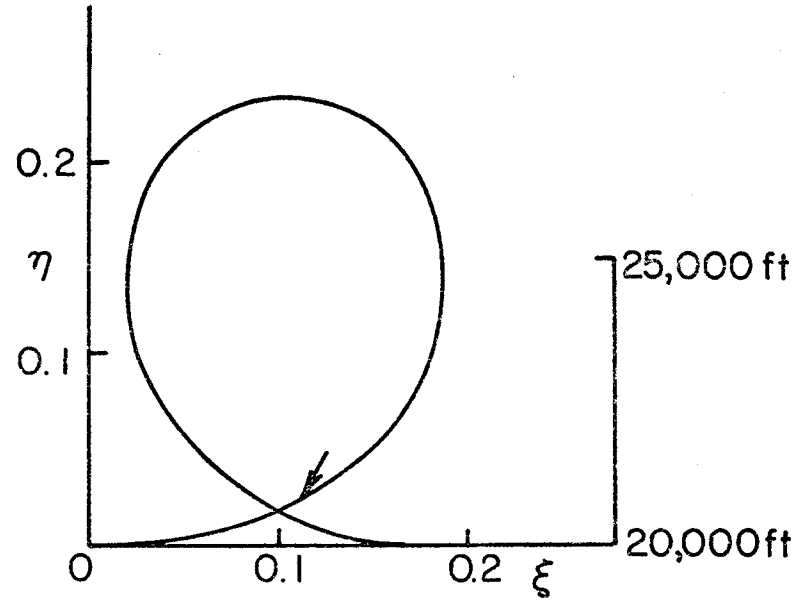


| | | | |
|---|---|---|---|
| Initial $C_L$ | | 0.4 | |
| Final Values | | | |
| Time | $t_f$ | 40.07 | sec |
| Speed | $M_f$ | 0.6961 | M |
| Range | $x_f$ | 5676 | ft |
| Altitude | $y_f$ | 0.47 | ft |
| Maximum Normal Acceleration | ↙ | 5.85 | g |

FIG. 16 HISTORY OF CONTROL AND STATE VARIABLES, LAGRANGE MULTIPLIERS: $C_{L_{MAX}} = 1.0$, $Tw_{MAX} = 0.5$, $\lambda_3 = -0.7391$, $\lambda_4 = 0.09551$

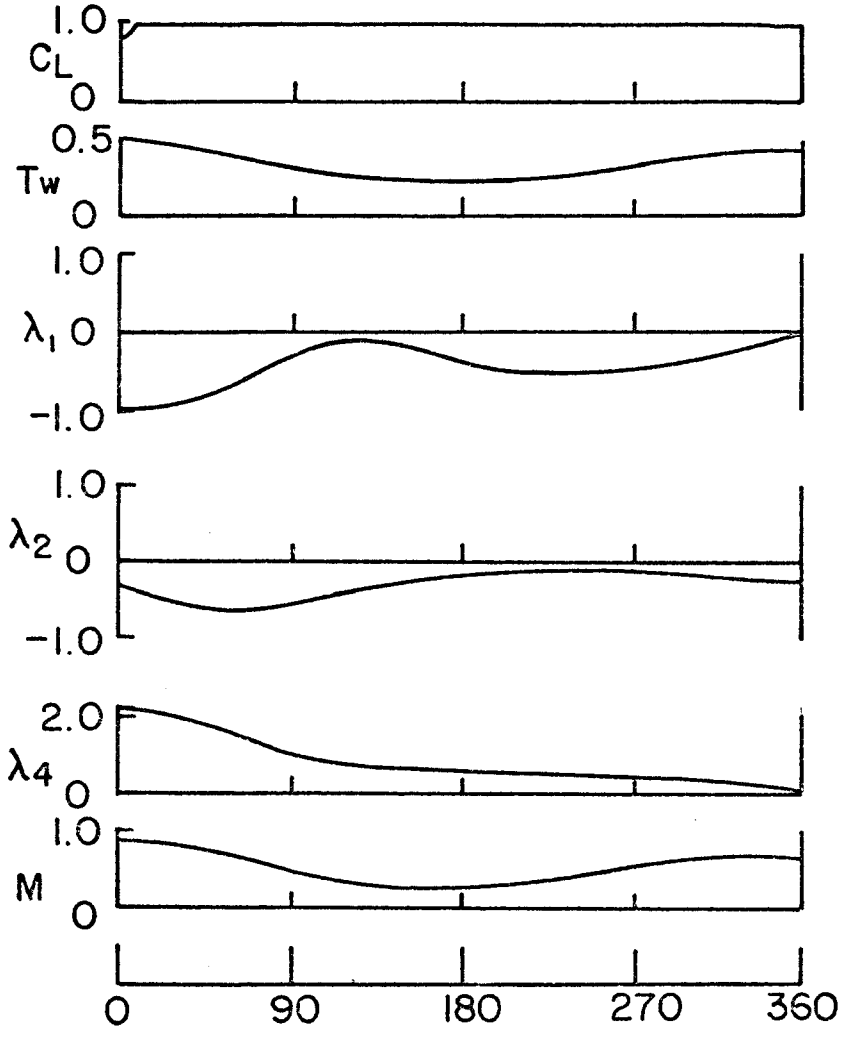


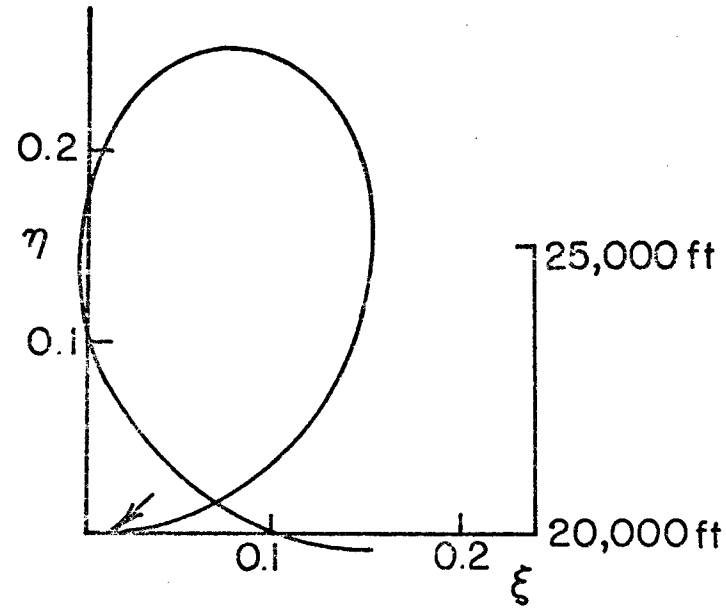


| | | | |
|---|---|---|---|
| Initial $C_L$ | | 0.8453 | |
| Final Values | | | |
| Time | $t_f$ | 47.51 | sec |
| Speed | $M_f$ | 0.6659 | M |
| Range | $x_f$ | 5257 | ft |
| Altitude | $y_f$ | -296.6 | ft |
| Maximum Normal Acceleration | ↙ | 6.53 | g |

FIG. 17 HISTORY OF CONTROL AND STATE VARIABLES, LAGRANGE MULTIPLIERS: $C_{L_{MAX}} = 1.0$, $(Tw_{MAX})_i = 0.5$, $\lambda_3 = 0$ (MORE REALISTIC CASE 1)

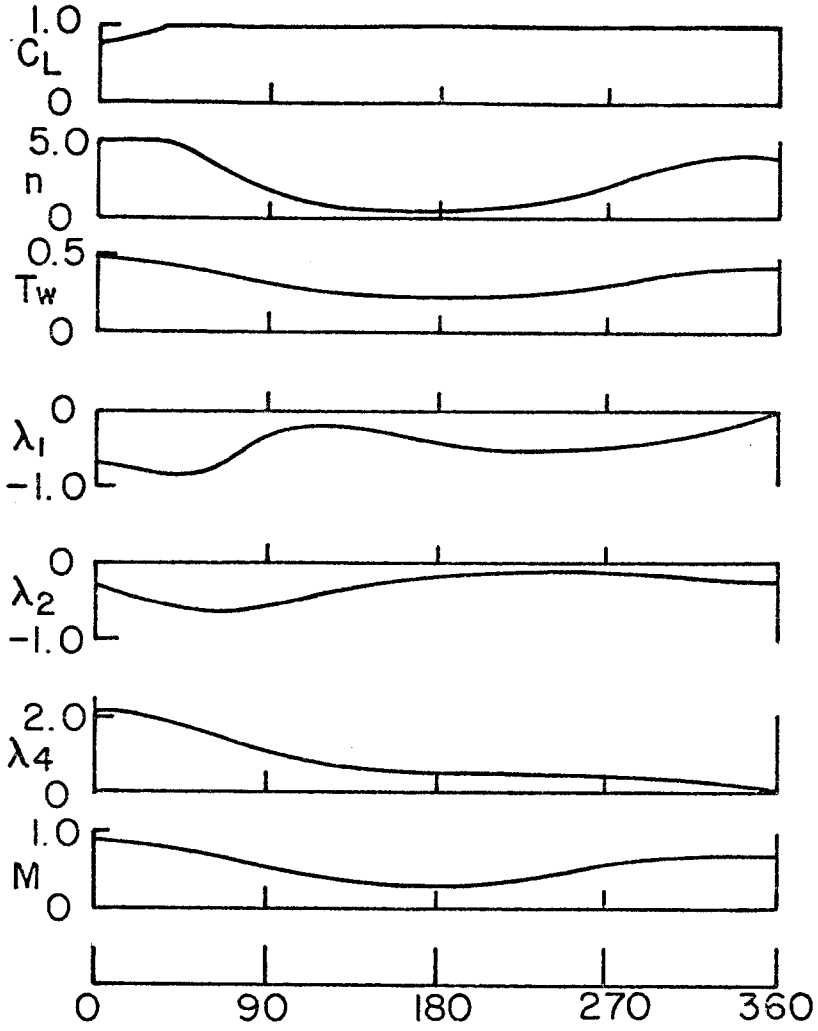


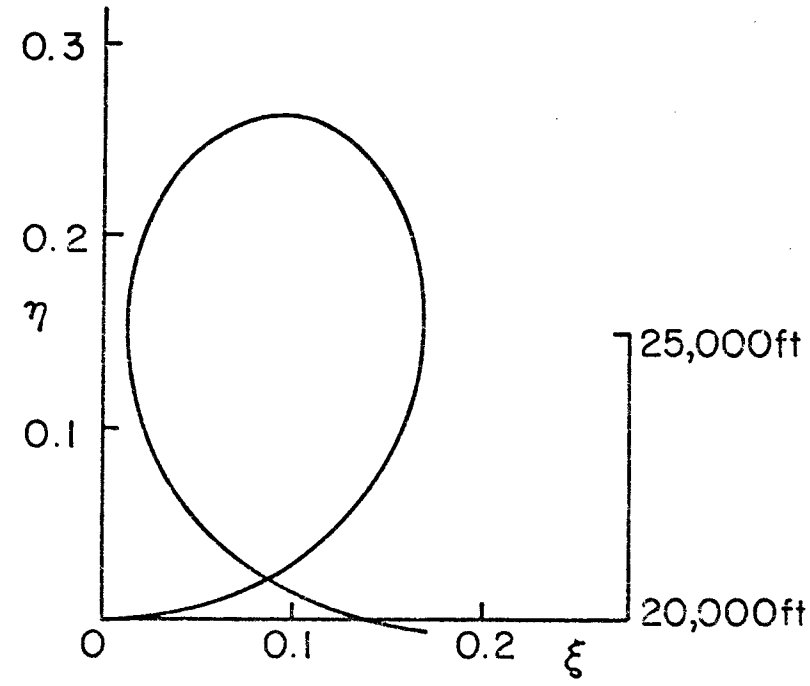


| | | | |
|---|---|---|---|
| Initial $C_L$ | | 0.7419 | |
| Final Values | | | |
| Time | $t_f$ | 48.03 | sec |
| Speed | M | 0.6716 | M |
| Range | $x_f$ | 5711 | ft |
| Altitude | $y_f$ | -125.4 | ft |

FIG. 18 HISTORY OF CONTROL AND STATE VARIABLES, LAGRANGE MULTIPLIERS: $C_{L\,MAX} = 1.0$, $n_{MAX} = 5.0$, $(T_{w_{MAX}})_i = 0.5$, $\lambda_3 = 0$ (MORE REALISTIC CASE 2)

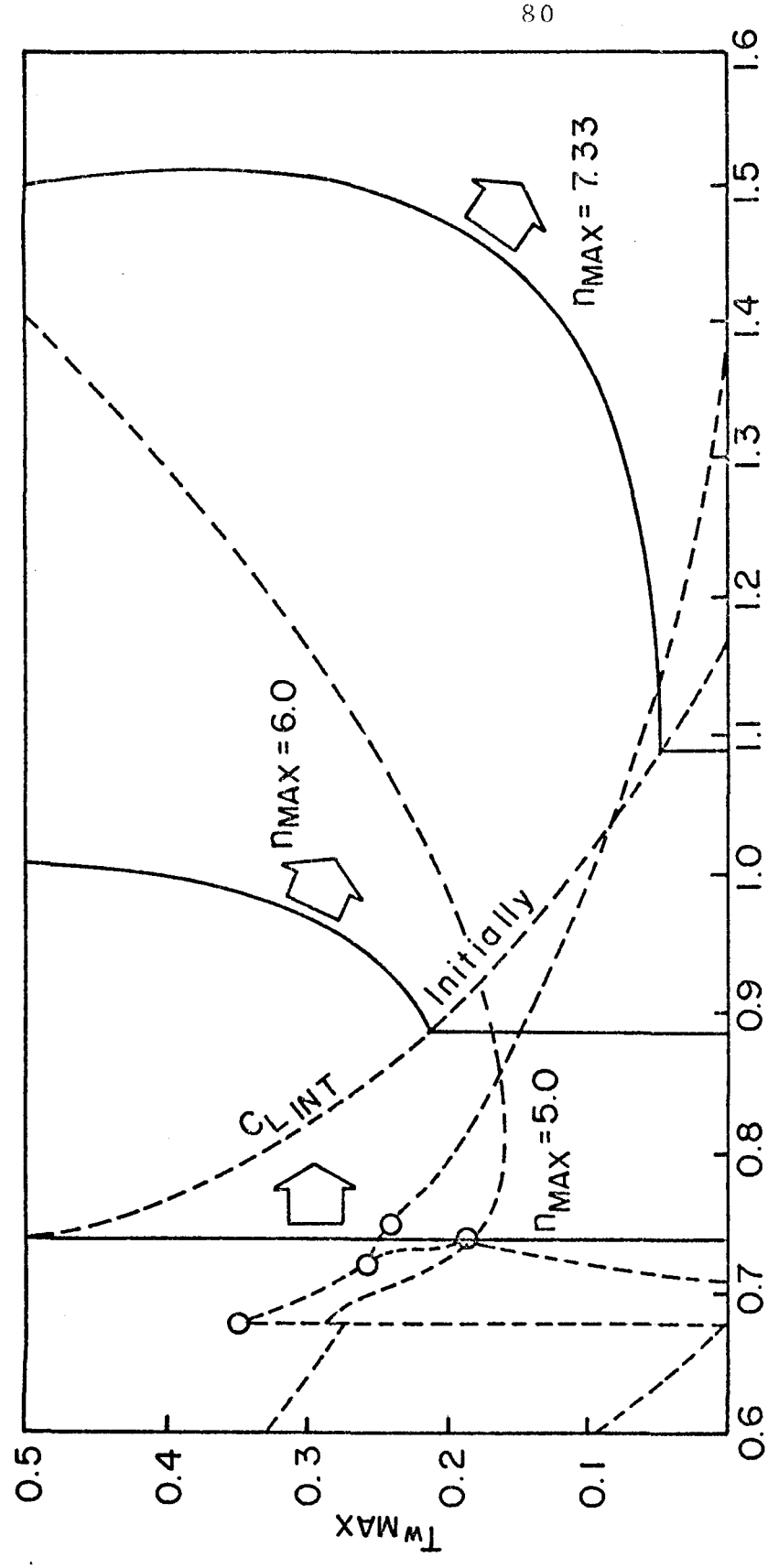


FIG. 19 ZONES OF INFLUENCE OF $n_{MAX}$ LIMITATION